



Heat transfer from a vertical bundle of serrated finned tubes in an air fluidized bed  
by Daniel Wade Vanderhoof

A thesis submitted in partial fulfillment of the requirements for the degree of MASTER OF SCIENCE  
in Chemical Engineering  
Montana State University  
© Copyright by Daniel Wade Vanderhoof (1978)

**Abstract:**

The objective of this investigation is to determine and present information on heat transfer from vertical bundles' of serrated fin tubes in an air fluidized bed. A cylindrical plexiglass column 14 inches in diameter and glass beads as the solid particles were used. The experimental variables were particle diameter (0.0076 inches to 0.0164 inches), air flow rate (63 pounds per hour to 564 pounds per hour), fin length. (0.125 inches to 0.344 inches), fin width (0.094 inches to 0.156 inches), number of rows per inch (6 to 10), number of fins per inch (86 to 250). The heat transfer coefficient increased with decreasing particle size and increasing flow rate. For some conditions a maximum heat transfer coefficient was observed with respect to flow rate. The heat transfer coefficient increased with increasing fin spacing and decreasing fin length. Gains as large as 74 percent, when compared to bare tubes, were obtained using the smallest particles and largest fin spacing.

STATEMENT OF PERMISSION TO COPY

In presenting this thesis in partial fulfillment of the requirements for an advanced degree at Montana State University, I agree that the Library shall make it freely available for inspection. I further agree that permission for extensive copying of this thesis for scholarly purposes may be granted by my major professor, or in his absence, by the Director of Libraries. It is understood that any copying or publication of this thesis for financial gain shall not be allowed without my written permission.

Signature Daniel W. Vanderloof

Date May 25, 1978

HEAT TRANSFER FROM A VERTICAL BUNDLE OF SERRATED FINNED TUBES  
IN AN AIR FLUIDIZED BED

by

DANIEL WADE VANDERHOOF

A thesis submitted in partial fulfillment  
of the requirements for the degree


of

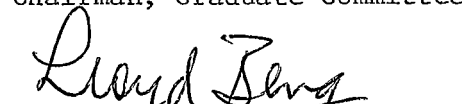
MASTER OF SCIENCE

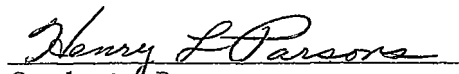
in

Chemical Engineering

Approved:

  
Chairman, Graduate Committee

  
Head, Major Department

  
Graduate Dean

MONTANA STATE UNIVERSITY  
Bozeman, Montana

May, 1978

ACKNOWLEDGMENT

The author wishes to thank the staff of the Chemical Engineering Department and his Graduate Committee for their time and effort.

Special acknowledgement is given to William Genetti for his assistance throughout the project.

The funding for this research was provided by the National Science Foundation.

## TABLE OF CONTENTS

	Page
VITA .....	ii
ACKNOWLEDGEMENTS .....	iii
LIST OF TABLES .....	vi
LIST OF FIGURES .....	vii
ABSTRACT .....	viii
INTRODUCTION .....	1
THEORY AND PREVIOUS RELATED RESEARCH .....	3
Mechanisms of Fluidization for Heat Transfer .....	3
Previous Related Research .....	5
EXPERIMENTAL PROGRAM .....	7
EXPERIMENTAL EQUIPMENT .....	9
Fluidizing System .....	9
Heater and Finned Tube Assemblies .....	11
Electrical System .....	13
EXPERIMENTAL PROCEDURE .....	18
Minimum Fluidization Determination .....	18
Procedure for a Typical Run .....	19
RESULTS AND DISCUSSION .....	21
Determination of Heat Transfer Coefficients .....	21
Effect of Mass Velocity on $h$ .....	24
Effect of Particle Size on $h$ .....	27
Effect of Fin Spacing on $h$ .....	27

	Page
Effect of Fin Length on h .....	28
Effect of Fin Separation on h .....	28
Effect of Tube Location on h .....	29
Performance of Finned Tubes .....	38
CONCLUSIONS .....	45
RECOMMENDATIONS .....	46
ERROR ANALYSIS .....	47
CALCULATIONS .....	48
Air Mass Velocity .....	48
Tube Temperatures .....	49
Bed Temperatures .....	49
Heat Input to Each Tube .....	49
Total Tube Area .....	49
Air Thermal Conductivity .....	50
Air Viscosity .....	50
Heat Transfer Coefficient .....	50
Particle Nusselt Number .....	51
Particle Reynolds Number .....	51
NOMENCLATURE .....	52
BIBLIOGRAPHY .....	54

## LIST OF TABLES

Table		Page
I	Range of Experimental Variables .....	8
II	Glass Bead Characteristics and Distribution.....	9
III	Finned Tube Dimensions .....	12
IV	Minimum Fluidizing Velocities .....	19

## LIST OF FIGURES

Figure		Page
1	Proposed Heat Transfer Mechanism .....	6
2	Schematic View of Equipment .....	14
3	Top View of Finned Tubes .....	15
4	Side View of Fin Tube .....	16
5	Details of Cartridge Heater .....	17
6	h Versus $Q/\Delta T$ , #4 Tubes .....	25
7	h Versus $Q/\Delta T$ , #5 Tubes .....	26
8	h Versus Air Mass Velocity, #1 Tubes .....	30
9	h Versus Air Mass Velocity, #2 Tubes .....	31
10	h Versus Air Mass Velocity, #3 Tubes .....	32
11	h Versus Air Mass Velocity, #4 Tubes .....	33
12	h Versus Air Mass Velocity, #5 Tubes .....	34
13	h Versus Air Mass Velocity, Small Particles .....	35
14	h Versus Air Mass Velocity, Medium Particles .....	36
15	h Versus Air Mass Velocity, Large Particles .....	37
16	p Versus Air Mass Velocity, #1 Tubes .....	40
17	p Versus Air Mass Velocity, #2 Tubes .....	41
18	p Versus Air Mass Velocity, #3 Tubes .....	42
19	p Versus Air Mass Velocity, #4 Tubes .....	43
20	p Versus Air Mass Velocity, #5 Tubes .....	44

## ABSTRACT

The objective of this investigation is to determine and present information on heat transfer from vertical bundles of serrated fin tubes in an air fluidized bed. A cylindrical plexiglass column 14 inches in diameter and glass beads as the solid particles were used. The experimental variables were particle diameter (0.0076 inches to 0.0164 inches), air flow rate (63 pounds per hour to 564 pounds per hour), fin length (0.125 inches to 0.344 inches), fin width (0.094 inches to 0.156 inches), number of rows per inch (6 to 10), number of fins per inch (86 to 250). The heat transfer coefficient increased with decreasing particle size and increasing flow rate. For some conditions a maximum heat transfer coefficient was observed with respect to flow rate. The heat transfer coefficient increased with increasing fin spacing and decreasing fin length. Gains as large as 74 percent, when compared to bare tubes, were obtained using the smallest particles and largest fin spacing.

## INTRODUCTION

Fluidized beds are used in a variety of industrial operations. Some of the applications are drying, calcining, mixing, coating and removal of fines from bed particles.

A fluidized bed consists of a column which contains solid particles that are supported by a porous distributor plate. A fluidizing mass, gas or liquid, flows upward through the distributor plate. At low mass velocities there is no movement of the solid particles. As the mass velocity is increased, the pressure drop across the bed of solid particles increases. When the pressure drop equals the weight of the solid particles, the bed will begin to expand. The mass velocity which causes this initial expansion is called the minimum fluidization velocity. The particles are separated and begin moving but there is no bubbling. Increasing the mass velocity increases the particle separation and movement and bubbles begin to rise up through the bed. As the bubbles rise they expand and burst upon reaching the top surface of the bed. The bed of solid particles resembles a "boiling liquid" (1).

The size and number of bubbles increase as the mass velocity increases. The bubbles agitate the bed and increase the random motion of the particles. The condition of free bubbling is known as aggregative fluidization and is encountered in most industrial applications. As the mass velocity is increased, the bubble size will grow until slugging occurs.

Some of the physical advantages of a fluidized bed are the uniform

temperature distribution, good solid mixing, high heat transfer coefficients between the bed and an immersed surface, the ability for continuous feed or recycle and good flexibility in the size and type of bed materials that can be used. The simplistic design with few moving parts results in lower capital and maintenance costs.

Some of the disadvantages of fluidized beds are erosion of column walls and immersed surfaces, solid particle degradation, difficulty in handling sticky materials and difficulty in accurately controlling residence time in continuous feed operations.

There are many applications where heat is extracted or added to the fluidized bed. Originally this was accomplished by heat transfer through the walls of the column. Because of the increased surface area bare tubes were immersed in the fluidized bed to increase the amount of heat transfer. A lot of work has been done to establish reliable design criteria for heat transfer from immersed surfaces. There has been some work done evaluating heat transfer from extended surfaces in fluidized beds. It has been possible to improve heat transfer rates with the use of extended surfaces. The purpose of this investigation is to determine and present information on the heat transfer from a bundle of vertically oriented serrated fin tubes.

## THEORY AND PREVIOUSLY RELATED RESEARCH

### Mechanism of Fluidization for Heat Transfer

The heat transfer coefficients from the bed to an appropriate surface are considerably larger than coefficients from a surface to a gas or a surface to a fixed bed. Several models based on different controlling heat transfer resistances have been developed to explain the higher heat transfer coefficients.

A "film" model developed by Levenspiel and Walton (2) describes a thin laminar film of fluidizing gas next to the surface which controls the rate of heat transfer. During fluidization the "scouring" action of the particles reduces the thickness of the laminar film thereby increasing the heat transfer rate.

A "packet" model was developed by Mickley and Fairbanks (3). This model describes "packets" of particles coming into contact with the heat transfer surface for short periods of time. The unsteady state heat conduction into the packet of particles is the controlling resistance. After staying near the surface for a short period of time the "packet" returns to the bulk of the bed and dissipates its energy.

The "particle" theory was developed by Ziegler, Koppel and Brazelton (4) and extended by Genetti and Knudsen (5). Assuming spherical particles of uniform diameter and that the physical properties of the solids and the fluids are constant, the theory proposes that particles from the bulk of the fluidized bed at the bulk medium temperature,  $T_b$ ,

move next to the heat transfer surface at temperature  $T_s$ . Energy is transferred by convection from the surrounding fluid for a short time period,  $\bar{\theta}$ . The fluid temperature is assumed to be the arithmetic mean of the surface temperature and the bulk medium temperature. After a short time the particle returns to the bulk medium where it dissipates its acquired energy. This mechanism is shown in Figure 1. The conduction heat transfer and radiation heat transfer from the surface to the particle are neglected. The following equation describes the heat transfer rate from an immersed surface in a fluidized bed.

$$Nu_p = hD_p = \frac{7.2}{\left[ 1 + \frac{6 k_g \bar{\theta}}{\rho_s C_{p_s} D_p^2} \right]^2} \quad (1)$$

$Nu_p$  = Particle Nusselt Number, Dimensionless

$h$  = Heat Transfer Coefficient,  $Btu/hr-ft^2-^{\circ}F$

$D_p$  = Particle Diameter, ft

$k_g$  = Fluid Thermal Conductivity,  $Btu/hr-ft-^{\circ}F$

$\bar{\theta}$  = Average Contact Time, hr

$\rho_s$  = Solid Particle Density,  $lbs/ft^3$

$C_{p_s}$  = Solid Particle Heat Capacity,  $Btu/lb-^{\circ}F$

Genetti and Knudsen extended the "particle" theory by recommend-

ing that 7.2 be substituted with  $10(1-\epsilon)^{0.48}$ , where  $(1-\epsilon)$  is the particle volume fraction. Kunii and Levenspiel (6) have compared models and suggested a general model which includes the different theories.

#### Previous Related Research

Heat transfer from an immersed surface to the solid particles has received a lot of attention in the past. Studies have been done to determine the effect of particle diameter, particle shape, density, heat capacity, fluid thermal conductivity, viscosity, void fraction and mass velocity. Chen and Withers (7,8) investigated heat transfer from vertically oriented bare and finned tubes in a fluidized bed. They varied fin height and fin spacing. They reported gains as large as 190 percent for heat transfer from helical copper fin tubes compared to plain tubes.

Bartel and Genetti (9) investigated the heat transfer from a horizontal bundle of carbon steel bare tubes and finned tubes. They varied fin height, tube spacing, particle diameter and mass velocity. Gains up to 80 percent, compared to bare tubes were reported. Priebe and Genetti (10), investigated heat transfer from horizontal serrated and spined tubes. For copper spines, gains as large as 60 percent were observed. Kratovil (11) investigated heat transfer from a horizontal bundle of continuous, helical copper finned tubes. Gains up to 190 percent were observed compared to bare tubes.

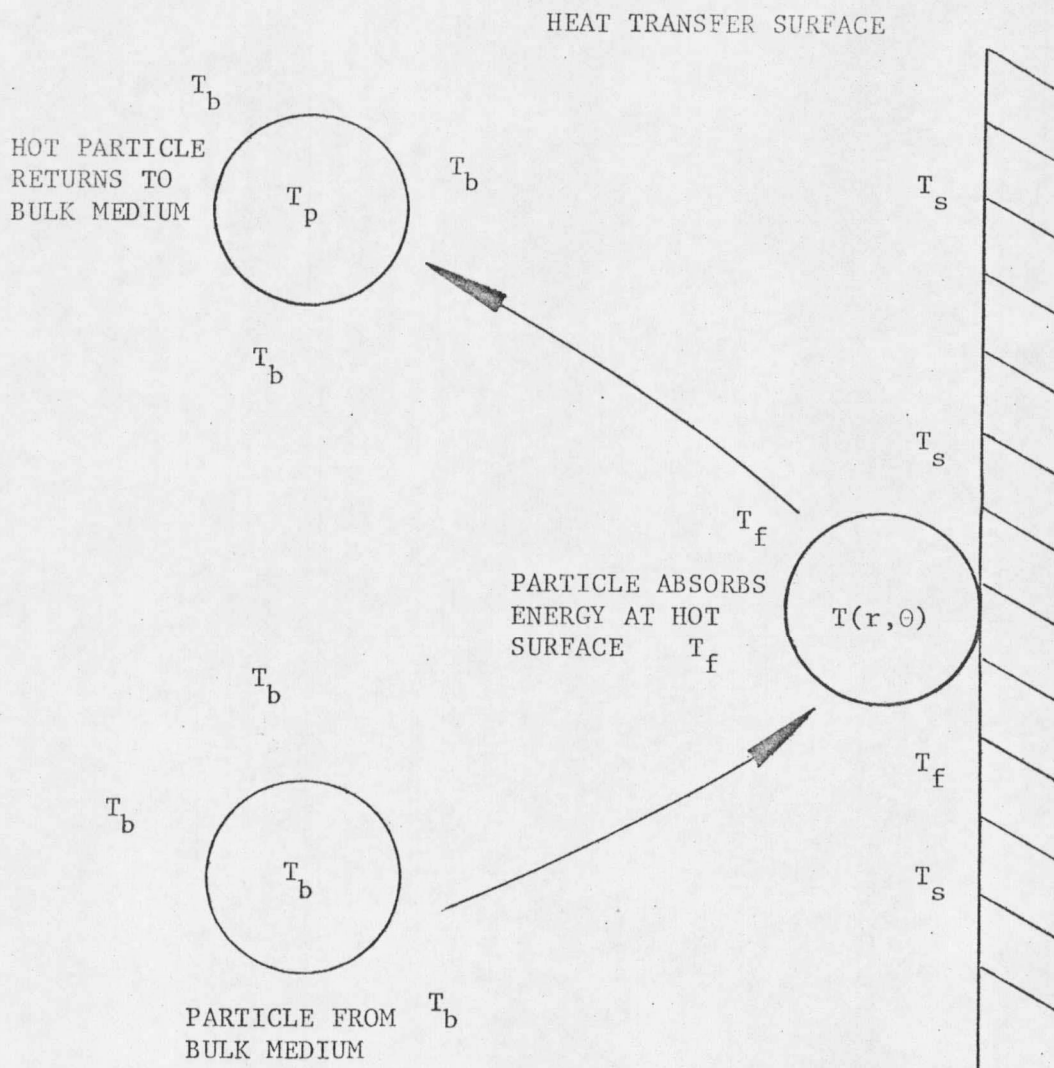


FIGURE 1. PROPOSED HEAT TRANSFER MECHANISM

## EXPERIMENTAL PROGRAM

The objective of this investigation was to determine the heat transfer coefficients of several bundles of serrated, or discontinuous, finned tubes oriented in the vertical position. The parameters that should affect the heat transfer coefficients are separated into three categories. First, the parameters of the fluidized bed. These are the solid particle size, shape and composition, and the physical properties of the fluidizing medium, the density, temperature, thermal conductivity and air viscosity. Second are the operating condition parameters. These are the fluidizing medium mass velocity and the static height of solid particles in the bed. Third are the parameters describing the geometry of the equipment. These are the size and shape of the column, and the dimensions and orientation of the finned tube bundles. The 6 experimental variables for this investigation were: particle diameter, air mass velocity, fin length, fin width, number of rows of fins per inch, and the number of fins per inch.

Air was used as the fluidizing medium. The inlet air temperature was in the range of  $100^{\circ}\text{F}$  to  $115^{\circ}\text{F}$ , and the physical properties of the inlet air were considered constant. Spherical glass beads were used as the solid particles. The density of the glass beads is approximately  $155 \text{ lbs/ft}^3$ . Electrical heaters were used as the heat source and 5 different tube bundles were investigated. Table I gives the range of experimental variables.

TABLE I. RANGE OF EXPERIMENTAL VARIABLES

Variable	Range
Particle Diameter	0.0076, 0.0109, 0.0164 Inch Diameter
Air Mass Velocity	63 to 564 lbs/hr-ft <sup>2</sup>
Fin Length	0.125, 0.188, 0.344 Inches
Fin Width	0.938, 0.156 Inches
Numbers of Rows/Inch	6.0, 8.0, 10.0
Number of Fins/Inch	85.7, 88.3, 14.49, 193.7, 250.3

## EXPERIMENTAL EQUIPMENT

### Fluidizing System

The main parts of the fluidizing system are the column, glass beads, distributor plate, funnel and air blower. A schematic drawing of the experimental equipment is shown in Figure 2.

The column was cylindrical and constructed of clear plexiglass that was 0.25 inches thick. The column was 13.5 inches inside diameter and 59 inches in height. A 0.75 inch thick flange was connected to the top and bottom of the column. One access port, 4 inches in diameter was located with its center 6 inches from the bottom of the column. The column was supported on a wooden frame which was bolted to the floor.

Three sizes of glass beads were used in this investigation. Their sizes and distributions were determined by Everly (9) and are listed in Table II.

TABLE II. GLASS BEADS CHARACTERISTICS AND DISTRIBUTION

Avg. Diameter (Inch)		Distribution (Inch)
Small	0.0076	0.005 - 0.0098
Medium	0.0109	0.0098 - 0.016
Large	0.0164	>0.016

The distributor plate consisted of two layers of a lightweight cotton cloth sandwiched between two layers of 100 mesh stainless steel wire cloth which was placed between two pieces of 0.03125 inch thick steel perforated plates. The perforations were 0.25 inches in diameter with a 0.5 inch center to center distance. The funnel was 13.5 inches in diameter at top and 2 inches in diameter at the bottom. It was 12 inches in height and constructed of 16 gauge galvanized steel. The spout of the funnel was 2 inches in diameter and 4 inches long. The distributor plate, fitted with rubber gaskets, and the funnel section were bolted to the bottom of the column using a 1 1/2 inch diameter wooden ring to reinforce the funnel. A 1 inch diameter drain pipe was fastened to the distributor plate and projected through the side of the funnel. The drain pipe was fitted with a gate valve. Two blowers were connected in parallel to the fluidized bed. The first blower was a size 4L Sutorbilt Blower driven by a 3 H.P. electrical motor. The blower fed into a 2 inch, schedule 40 pipe which was connected to the funnel with a flexible rubber hose. The air flow rate was regulated by adjusting a gate valve in a 2 inch bypass line. The air flow rate was measured by using a 1.5 inch orifice with vena contracta taps and a water filled manometer. The second blower was a Sutorbilt Blower driven by a 7.5 H.P. electrical motor. The second blower fed into a 2.5 inch schedule 40 steel pipe before reaching the column. The pipes from the two blowers were connected directly below the funnel section. The air flow

rate was regulated by adjusting a gate valve in a 2 inch bypass line. The air flow rate was measured using a 1.5 inch orifice with vena contracta taps and a water filled manometer. Gate valves were installed in the two air lines so the blowers could be operated independently.

#### Heater and Finned Tube Assemblies

Watlow Firerod Cartridge Heaters were used as the heat source in this investigation. As shown in Figure 5, each cartridge was 10 inches long, comprised of a heated section 6.5 inches long and two insulated ends. The finned tubes were 6.5 inches long and outside diameter was 0.625 inches. The heaters were inserted into the finned tubes with the two insulated ends protruding and a set screw in the wall of the tubes was tightened down so the heater could not slip. The bottom end of the heater was inserted into a copper pipe 9.125 inches long and 0.5 inch inside diameter. The other end of the heater, with the lead wires, was inserted into a similar copper pipe 52 inches long. The opposite ends of the two copper pipes were inserted into holes in the distributor plate and the top perforated plate holding the tubes in a vertical position. All the investigations were done with bundles of 7 finned tubes. A bundle configuration with one tube in the center of the bed and the other 6 tubes equally spaced around the center tube was used. The center distances between the outside tubes and the center tube, and between adjacent outer tubes was 2 inches. A total of 5 different sizes of

finned tubes were investigated. The surface areas and various dimensions are given in Table III. A top view and a side view of the fin tubes are shown in Figure 3 and Figure 4.

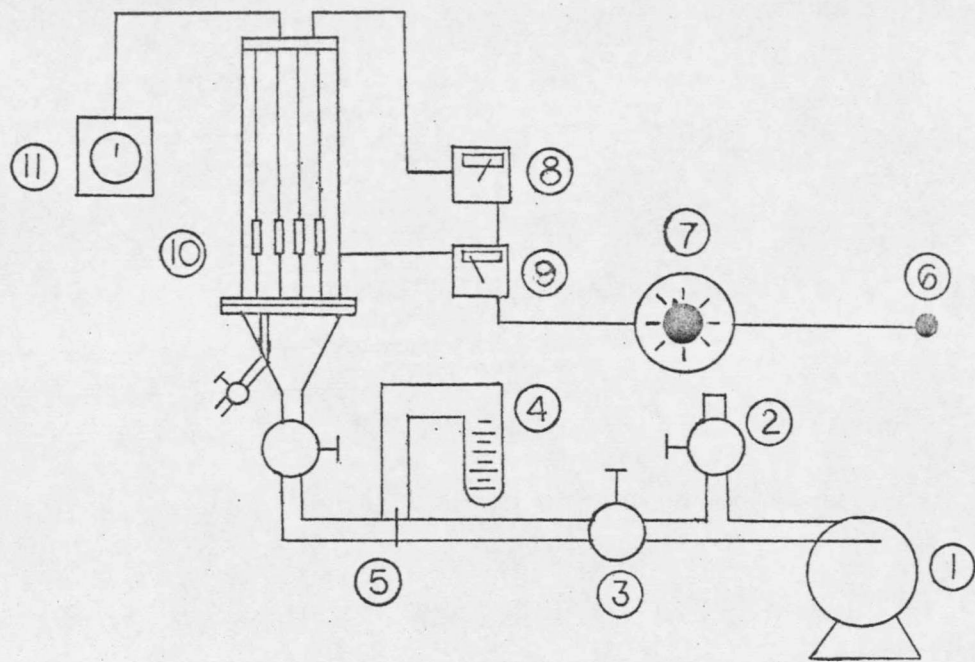
TABLE III. FINNED TUBE DIMENSIONS

	(Fin length, width, thickness, spacing in inches)				
	(All areas in Ft <sup>2</sup> )				
	#1 Tubes	#2 Tubes	#3 Tubes	#4 Tubes	#5 Tubes
Fin Length	0.188	0.188	0.188	0.344	0.125
Fin Width	0.094	0.094	0.094	0.156	0.156
Fin Thickness	0.031	0.031	0.031	0.025	0.0156
Fin Spacing	0.135	0.094	0.069	0.100	0.109
Rows/Inch	6.0	8.0	10.0	8.0	8.0
Total Area	0.395	0.498	0.618	0.571	0.260
Fin Area	0.326	0.436	0.563	0.497	0.181
Tube Area	0.069	0.062	0.055	0.007	0.079
Avg. No. of Fins	942	1269	1627	557	574

Electrical System

A single thermocouple was attached to the surface of each finned tube midway along the length. The thermocouple wires and heater lead wires were threaded up inside the copper pipe, out of the column, and to their respective panels. One thermocouple was used to measure the bed temperature in three different locations. The three thermowells were located 11.5 inches above the distributor plate and were equally spaced around the circumference of the bed. The thermowells projected 3 inches into the bed. The lead wires from the 8 thermocouples were plugged into a panel board which was wired to a switch box. A Model 156X15-P Brown Potentiometer was used to measure the temperature directly.

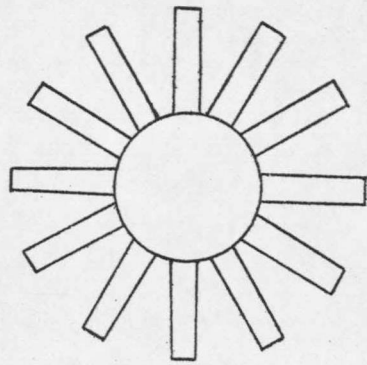
The electrical heaters in each tube were connected to a Simpson Model 390 Wattmeter and then to the electrical power supply. The heaters were connected in parallel and the wattmeter was connected so the wattage to the individual heaters could be measured by flipping the appropriate toggle switch. The power was supplied from a 110 volt AC line through a Powerstat and a Fenwall Model 524 high limit controller.



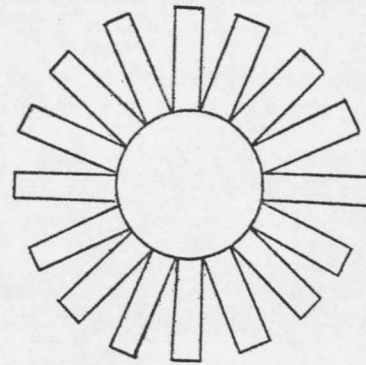
1. Air Blower 2. Bypass valve, 3. Main Air Line Valve, 4. Manometer,  
 5. Orifice, 6. Power Source, 7. Powerstat, 8. Wattmeter, 9. High  
 Temperature Limit Controller, 10. Plexiglass Column, 11. Potentiometer

FIGURE 2. SCHEMATIC VIEW OF EQUIPMENT

← OFD →



Tubes #4, #5



Tubes #1, #2, #3

FIGURE 3. TOP VIEW OF FINNED TUBES

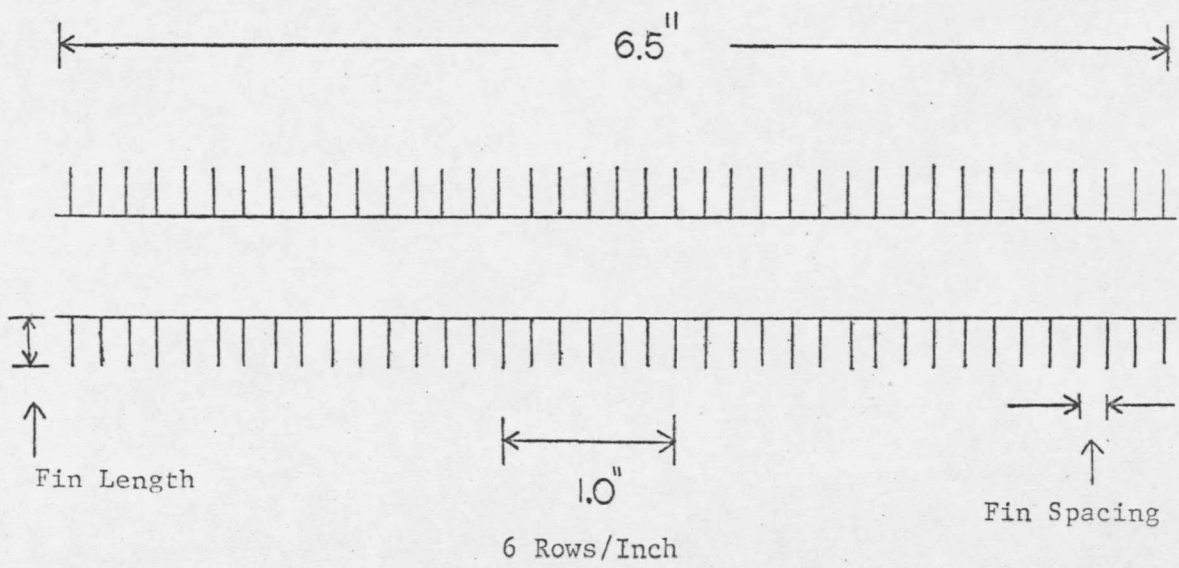


FIGURE 4. SIDE VIEW OF FIN TUBE

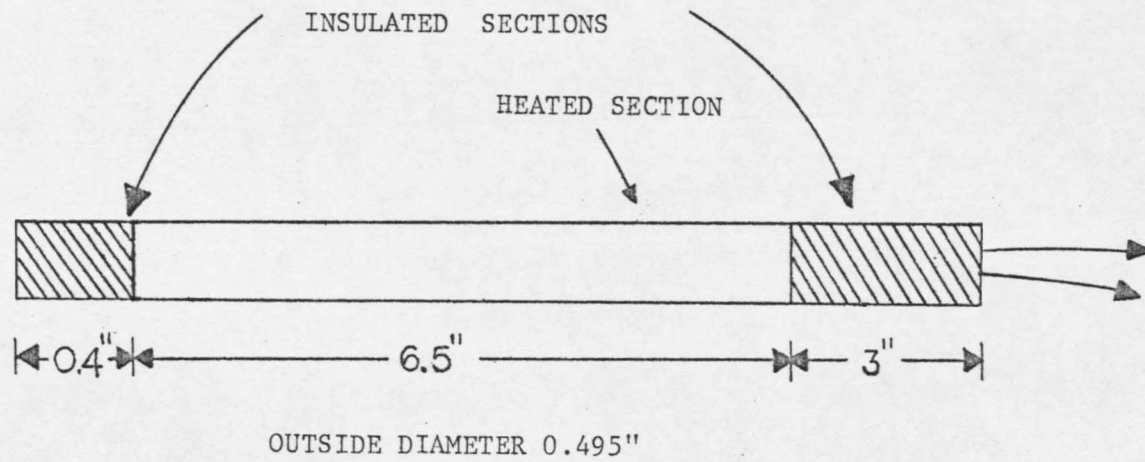


FIGURE 5. DETAILS OF CARTRIDGE HEATER

## EXPERIMENTAL PROCEDURE

### Minimum Fluidization Determination

The first experimental work performed in this investigation was to determine the minimum fluidizing velocities for the three particle sizes. The minimum velocities were determined by visual observation of the bed. The particles of the desired diameter were poured into the top of the column until a static height of 18 inches above the distributor plate were attained. The number one blower was used for the smallest particles and the number two blower was used for the other two particle sizes. The appropriate blower was turned on and the air flow rate was regulated until the bed was bubbling freely. The heaters were turned on and the bed was operated for 2-3 hours before reaching normal operating temperature. Then the air flow rate was regulated until the bed was just beginning to expand. A water-filled micromanometer was used to measure the pressure drop across the orifice. The observations were repeated several times from the direction of increasing as well as decreasing flow rate. The experimental minimum fluidizing velocities for the three particle sizes are shown in Table IV.

TABLE IV. MINIMUM FLUIDIZING VELOCITIES

Bead Size (Inches)	Minimum Fluidizing Velocity (lbs/hr/ft <sup>2</sup> )
.0076	62.8
.0109	63.7
.0164	125.3

Procedure for a Typical Run

The finned tubes to be investigated were chosen, the thermocouples were attached to each of the 7 tubes and a heater was inserted and fastened to each tube. The copper pipes used to hold the tube assemblies were put into the bed. The heater lead wires and thermocouple wires were threaded into the upper copper pipe and connected to their respective panels. The ends of the heaters were inserted into the copper pipes and the end of the copper pipes were fastened down so they would not come loose during operation of the bed. One of the particle sizes was selected and the column was filled to a static height of 18 inches. The appropriate blower was turned on and the valve in the bypass line was adjusted to regulate the air flow rate to two times the minimum fluidizing velocity. The power to the heaters was turned on and adjusted to a level of 200 watts per heater. The column was allowed to operate for 4 hours to reach steady state operating conditions. The temperatures of

the tubes and bed, wattage, air inlet conditions and pressure drop across the orifice were recorded. The column was allowed to operate for another hour and readings were taken again. For subsequent runs the valve in the bypass line was adjusted to get the desired flow rate and the column was operated for 2 hours to reach steady state. The temperatures, wattage, air inlet conditions and pressure drop were recorded again. The column was operated for another hour before taking a second set of readings. This procedure was repeated until all of the desired flow rates had been investigated.

The column was shut down and the particles were drained out through the 1 inch drain pipe. The access port was opened and a vacuum cleaner was used to remove any remaining beads from the distributor plate and the walls of the column. The drain pipe and access port were closed and the next particle size was loaded into the column as described previously. After all 3 particle sizes were investigated, the finned tubes were replaced and the procedure was repeated until all 5 fin. tube bundles had been investigated.

## RESULTS AND DISCUSSION

### Determination of Heat Transfer Coefficients

A single thermocouple was attached to the surface of each tube in the bundle. The thermocouple was used to measure the temperature at the base of the fin. Since there will be a temperature distribution along the length of the fin, this temperature can not be used to determine the heat transfer coefficient.

To determine the temperature distribution in the fin, an energy balance was taken about a differential element. The temperature across the width, and the thickness were assumed constant. The following procedure was used to solve for the temperature distribution:

1. The heat conducted into the element at  $x$  was set equal to the heat conducted out of the element at  $x + \Delta x$  plus the heat loss by convection from the surface.

$$-k w v \left. \frac{dT}{dx} \right|_x = -k w v \left. \frac{dT}{dx} \right|_{x+\Delta x} + h w v (T - T_b) \Delta x \quad (2)$$

where

$k$  = Thermal conductivity of the fin, Btu/hr-ft-<sup>o</sup>F

$w$  = Fin width, ft

$v$  = Fin thickness, ft

$h$  = Average heat transfer coefficient, Btu/hr-ft<sup>2</sup>-<sup>o</sup>F

substituting  $\theta$  for  $(T - T_b)$  and rearranging

$$\frac{d^2\theta}{dx^2} - \frac{2(w+v)}{wv} \frac{h}{k} \theta = 0 \quad (3)$$

the boundary conditions are:

$$a) \quad x = 0 \quad \theta = (T_w - T_b) \quad (4)$$

$$x = L \quad \left. \frac{d\theta}{dx} = \frac{-h}{k} \theta \right|_L \quad (5)$$

For the #1, #2 and #3 finned tubes the second order differential equation was solved numerically to determine the temperature distribution in the fin.

2. Once the temperature distribution was determined the mean temperature of the fin was calculated. The heat transfer coefficients were then determined using the following equation:

$$h = q / \left( (T_w - T_b)(A_b) + (T - T_b)_{MF} A_F \right) \quad (6)$$

$h$  = Heat transfer coefficient, Btu/hr-ft<sup>2</sup>-°F

$q$  = Heat input per tube, Btu/hr

$A_b$  = Bare tube area, ft<sup>2</sup>

$A_f$  = Fin area, ft<sup>2</sup>

$T_w - T_b$  = Wall temperature minus bed temperature, °F

$(T - T_b)_{MF}$  = Mean fin temperature minus bed temperature, °F

3. For the #4 and #5 finned tubes, the second order differential equation was solved analytically. The solution was of the form:  $\theta = A \sinh(Cx) + B \cosh(Cx)$  (7)

$$\text{where } C^2 = \frac{2(w+v)}{wv} \frac{h}{k} \quad (8)$$

Applying the two boundary conditions to solve for the constants A and B gave the following temperature distribution:

$$\theta(x) = T - T_b = \frac{(T_w - T_b) \left[ C \sinh(CL) + \frac{h}{k} \cosh(CL) \right] \sinh(Cx) + (T_w - T_b) \cosh(Cx)}{C \cosh(CL) + \frac{h}{k} \sinh(CL)} \quad (9)$$

4. The heat transferred to each fin was determined by the following equation:

$$q_{\text{Fin}} = h \cdot 2(w+v) \int_{X=0}^{X=L} \theta(x) dx \quad (10)$$

which gave:

$$q_{\text{Fin}} = \frac{k w v (T_w - T_b) C \left[ C \sinh(CL) + \frac{h}{k} \cosh(CL) \right]}{\frac{h}{k} \sinh(CL) + C \cosh(CL)} \quad (11)$$

5. To obtain a relationship between the amount of heat transferred and the heat transfer coefficient, the above equation was divided by  $(T_w - T_b)$  and multiplied by the total number of fins per tube,  $N_t$ . The heat transferred from the bare portion must be added to get the total heat transferred.

$$\frac{Q}{\Delta T} = N_t \frac{k w v C \left[ C \sinh(CL) + \frac{h}{k} \cosh(CL) \right] + A_b h}{\frac{h}{k} \sinh(CL) + C \cosh(CL)} \quad (12)$$

Q = The total heat transferred, Btu/hr

$$\Delta T = T_w - T_b, \text{ } ^\circ\text{F}$$

$$A_b = \text{Bare tube area, ft}^2$$

The heat transfer coefficient was then plotted versus  $Q/\Delta T$ .

The graphs for the #4 and #5 tubes are shown in Figures and

. The heat transfer coefficients versus  $Q/\Delta T$  were also plotted for the #1, #2, and #3 finned tubes. Several of the heat transfer coefficients from the analytical solution were compared to the results of the numerical solution. Since there was less than 2% error when comparing the two solutions, the heat transfer coefficients were not determined using the analytical solution.

This method of calculating the heat transfer coefficients assumes that the heat transfer coefficient remains constant over the entire surface.

#### Effect of Mass Velocity on h

As the mass velocity was increased, h generally increased, sometimes reached a maximum and then decreased. The maximum occurs because of two opposite effects. With the increased mass velocity there is increased particle movement which results in shorter particle-surface residence times and higher coefficients. With the increased mass velocity there is also a higher void fraction which reduces the particle

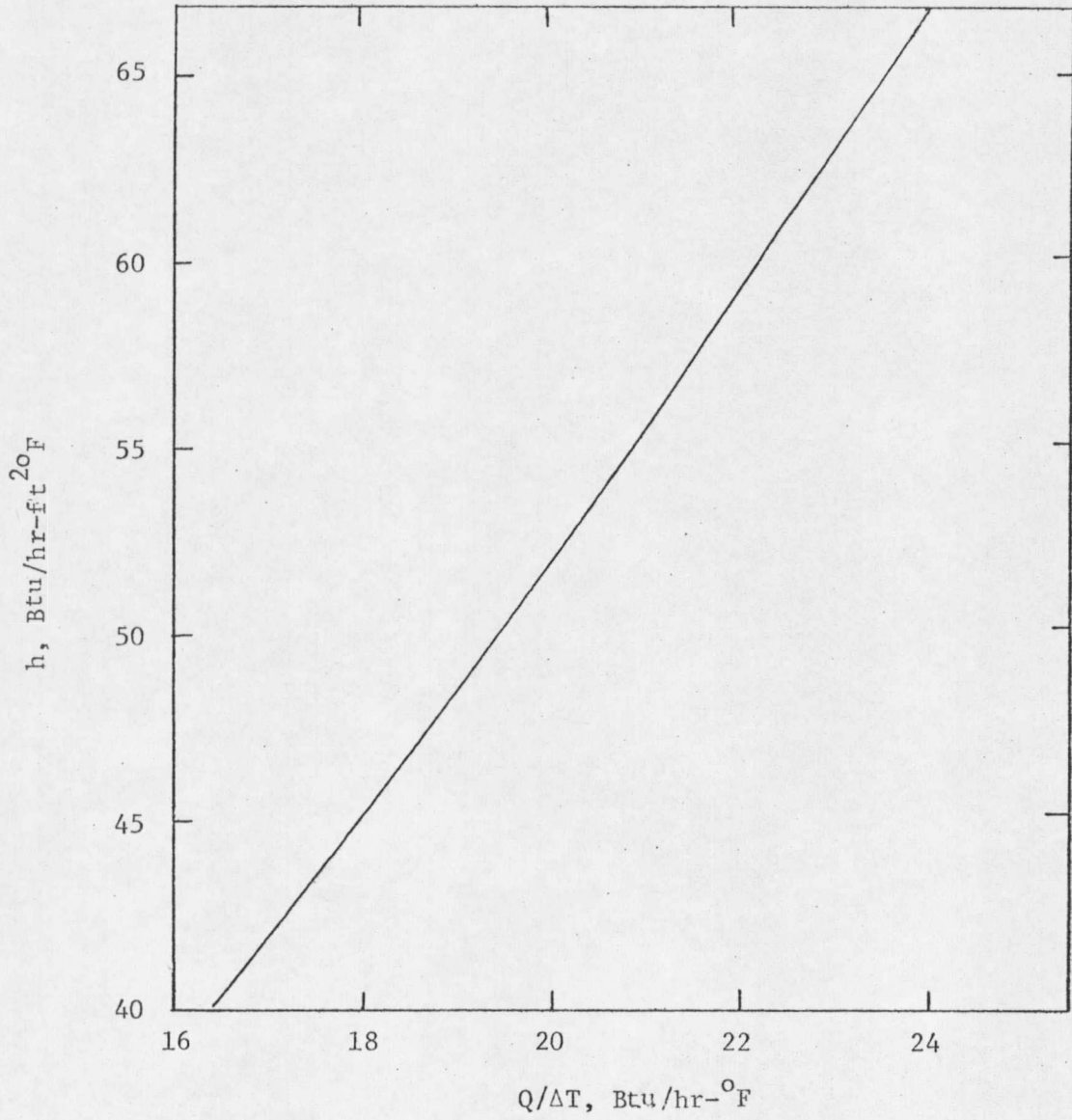


FIGURE 6.  $h$  VERSUS  $Q/\Delta T$ , #4 TUBES

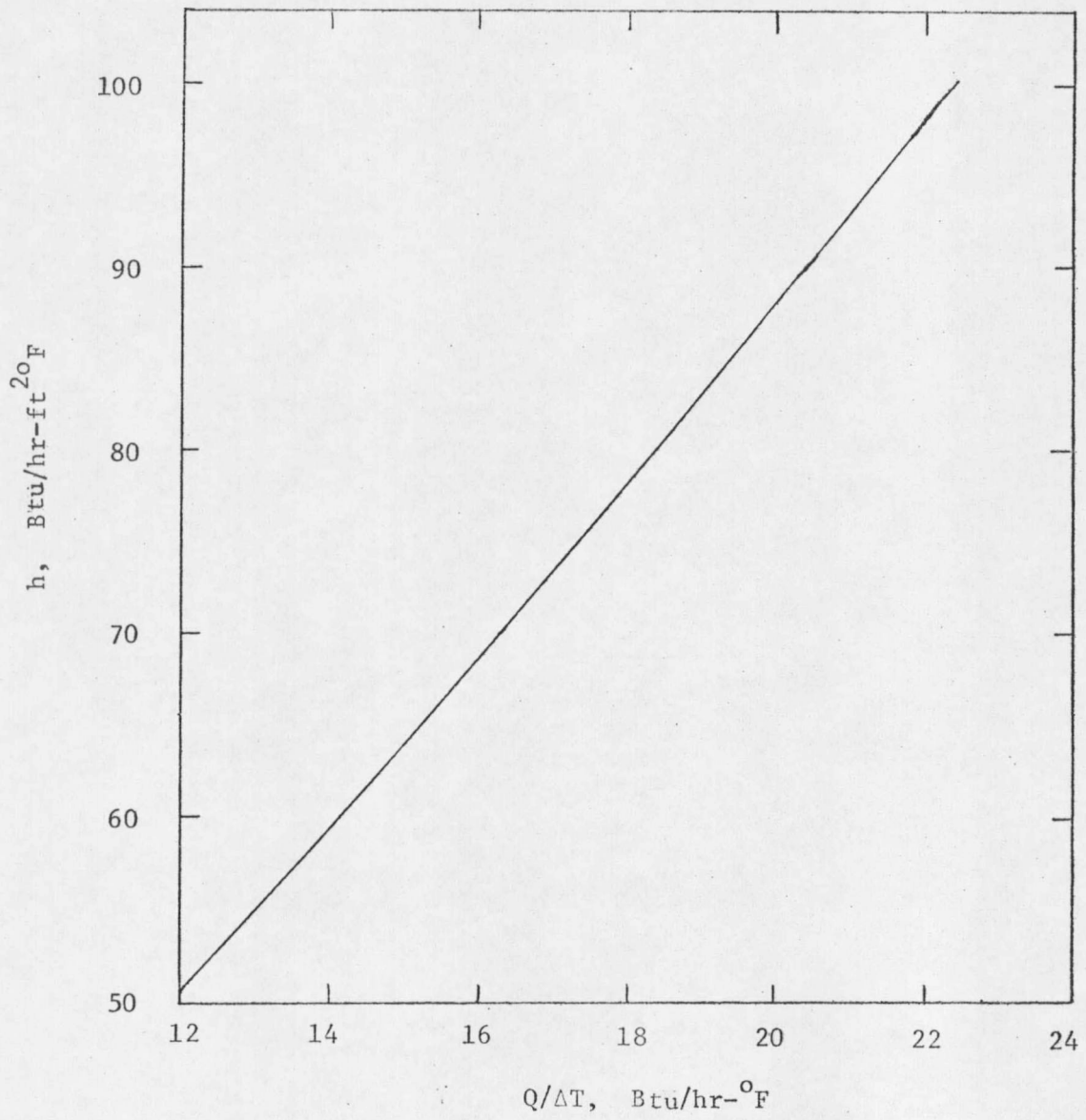


FIGURE 7.  $h$  VERSUS  $Q/\Delta T$ , #5 TUBES

concentration next to the surface and reduces the coefficients.

In this investigation the plots of  $h$  versus air mass velocity for the small particles generally had the steepest positive slopes, followed by the slopes of the plots for the medium particles, followed by the slopes of the plots for the large particles. Maximum coefficients were reached with all three particle sizes. The values of  $h$  are plotted versus air mass velocity for the different finned tubes in Figures 8, 9, 10, 11, and 12.

#### Effect of Particle Size on $h$

The heat transfer coefficient increased with decreasing particle size. The increase was larger between the large and medium particles than between the medium and small particles. There were increases of up to 44 percent in  $h$  between the large and small particles. The dependence of  $h$  on particle size was lessened with decreasing fin spacing and increasing fin length.

#### Effect of Fin Spacing on $h$

The coefficients decreased with decreasing fin spacing. With a smaller fin spacing it would be harder for the particles to move into and out of the regions close to the tube wall. The inner regions are not utilized as much as the outer regions resulting in lower coefficients. Tubes #1, #2, and #3 are identical except for fin spacing. The

#1 tubes have 6 rows of fins per inch, the #2 tubes have 8 rows of fins per inch and the #3 tubes have 10 rows of fins per inch. The effect of fin spacing on  $h$  can be seen in Figures 13, 14, and 15.

#### Effect of Fin Length on $h$

The heat transfer coefficient increased with decreasing fin length. With the longer fins the particles have a difficult time moving into and out of the regions close to the tube wall. The inner regions are not utilized as much as the outer regions resulting in lower coefficients. Tubes #4 and #5 differ primarily in fin length. The #4 tubes had a fin length of 0.344 inches and the #5 tubes had a fin length of 0.125 inches. The effect of fin length can be seen in Figures 13 and 15.

#### Effect of Fin Separation on $h$

The fin separation is the distance between adjacent fins in the same row. The fin separation is measured at the base of the fin next to the tube wall. Tubes #1, #2, and #3 had no fin separation and tubes #4 and #5 had a fin separation of 0.047 inches. With the small particles the fin separation is approximately 6 particle diameters and with the large particle approximately 3 particle diameters. This effect can be seen in Figures 13, 14, and 15.

Effect of Tube Location on h

The heat transfer coefficients for the individual tubes were compared to determine the effect of tube location on  $h$ . The variation of  $h$  was less than the experimental error and it was concluded that the tube location did not have an effect on  $h$ .

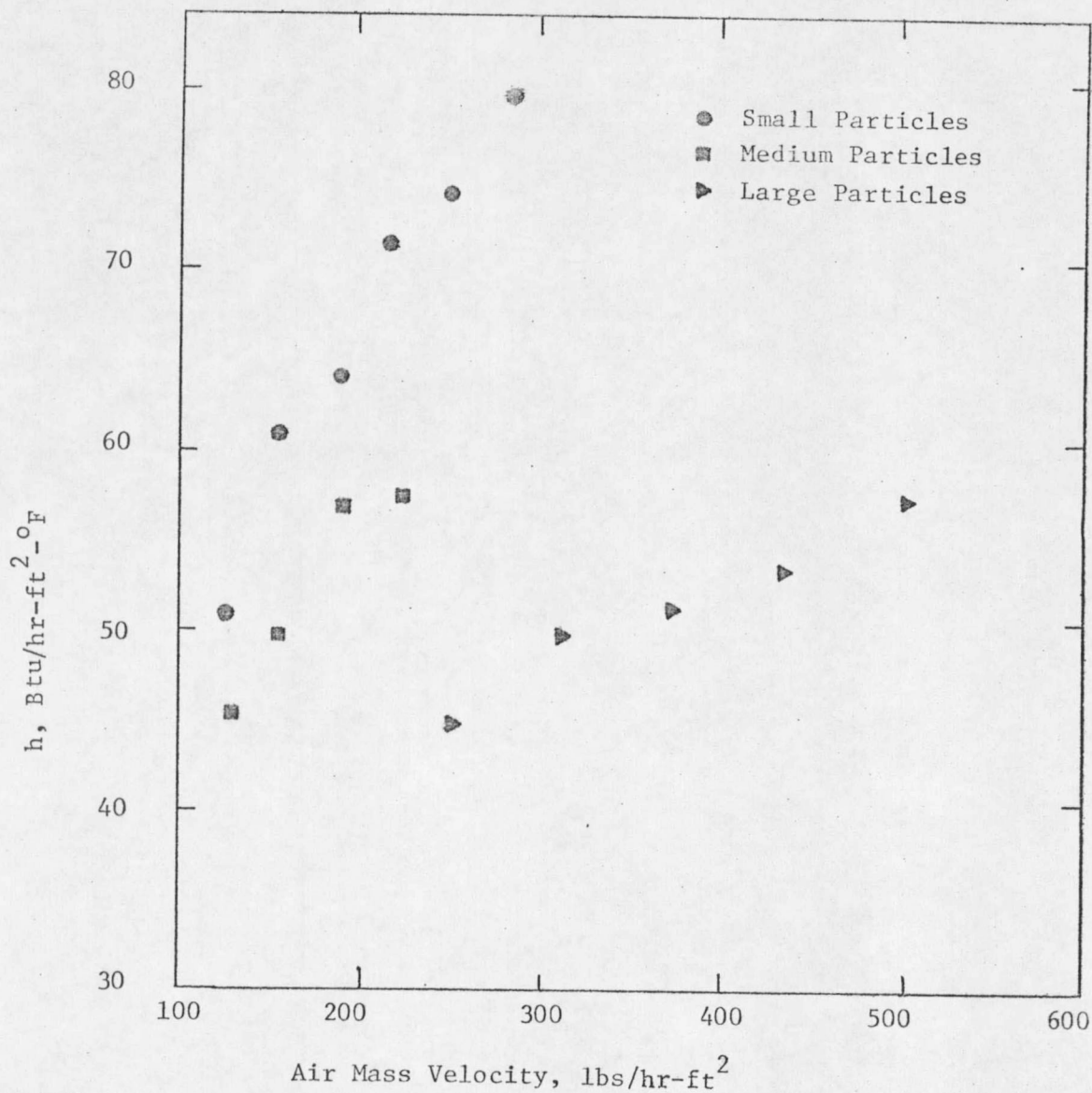


FIGURE 8.  $h$  VERSUS AIR MASS VELOCITY, #1 TUBES

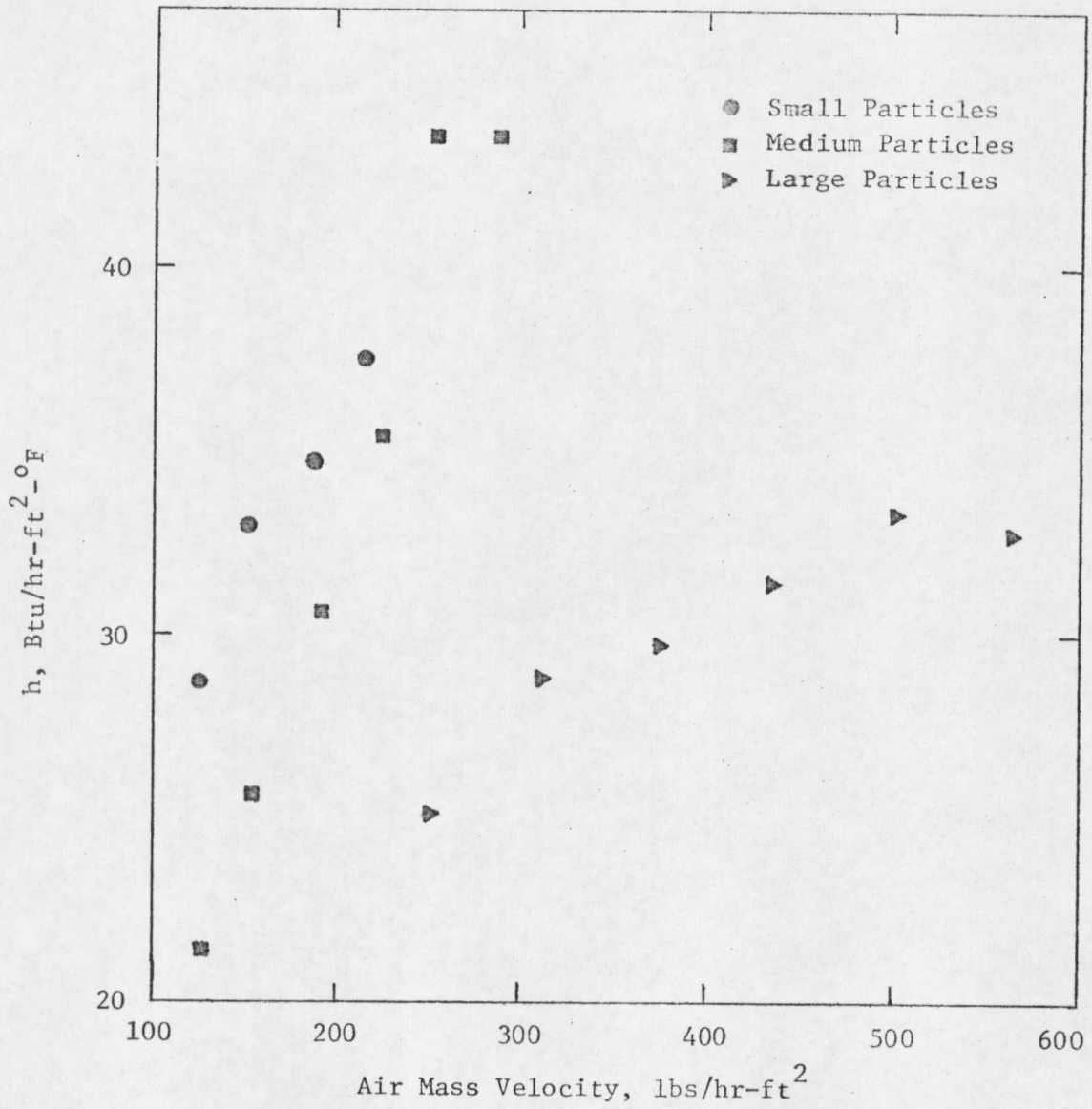


FIGURE 9.  $h$  VERSUS AIR MASS VELOCITY, #2 TUBES

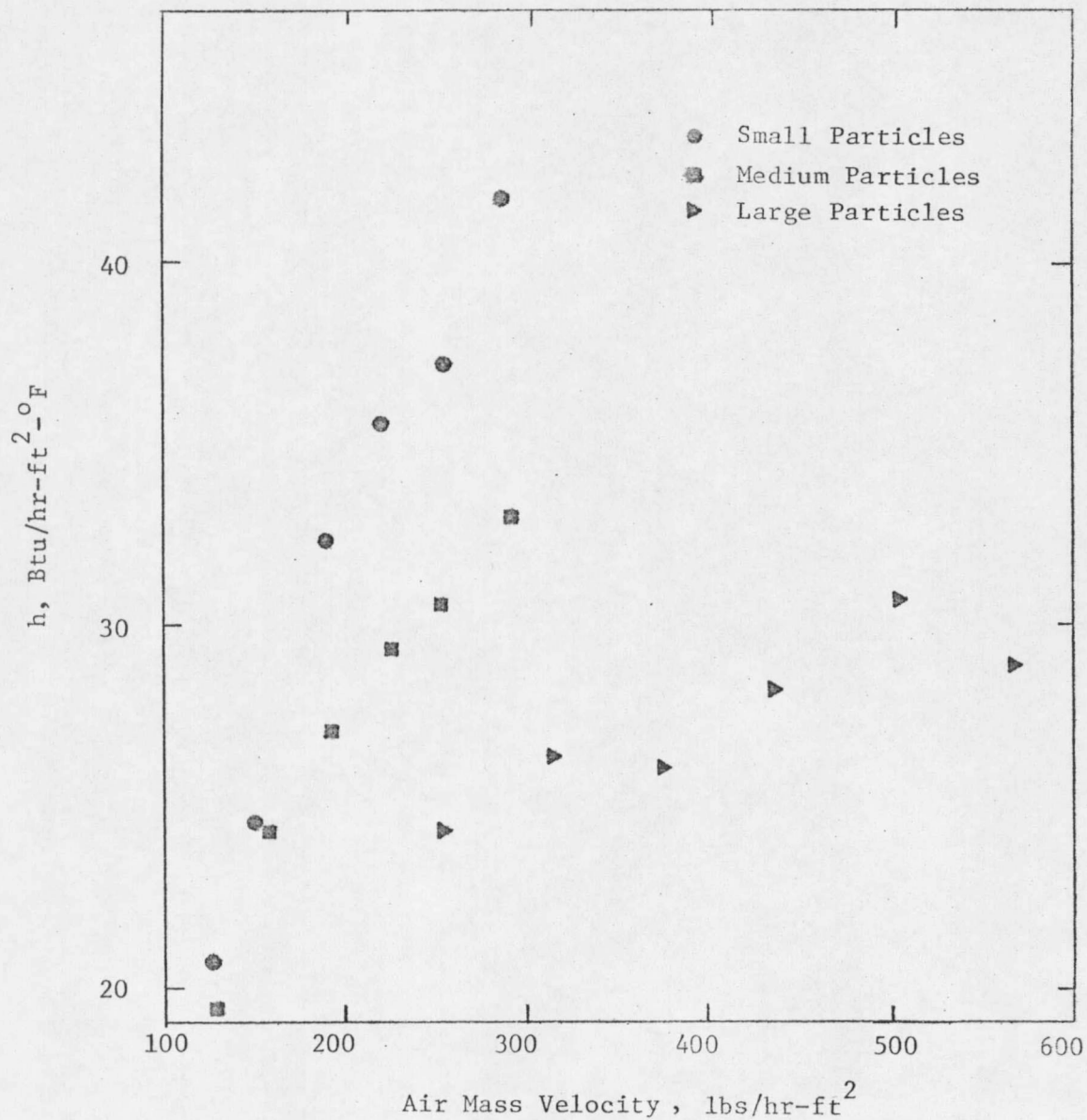


FIGURE 10.  $h$  VERSUS AIR MASS VELOCITY, #3 TUBES

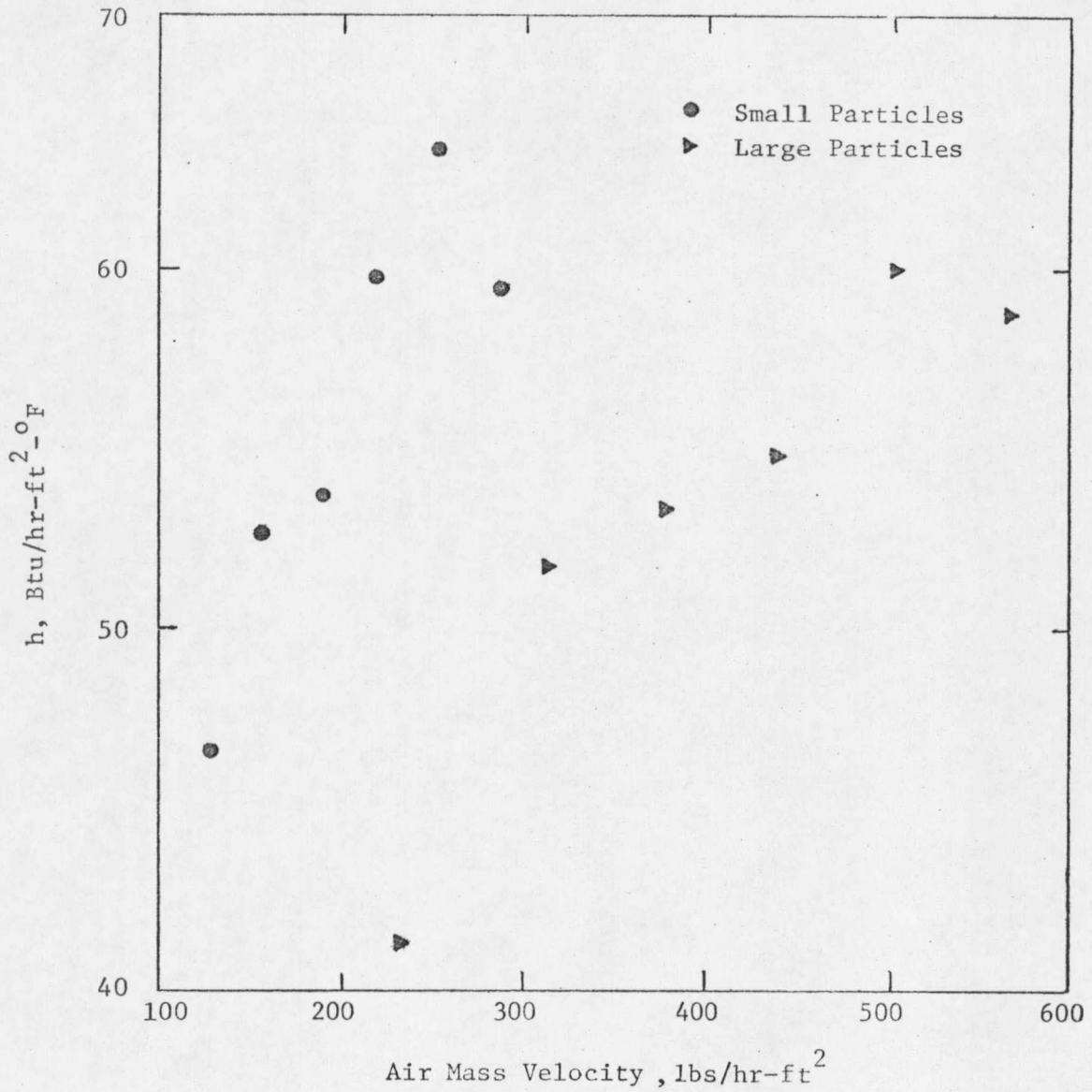


FIGURE 11.  $h$  VERSUS AIR MASS VELOCITY, #4 TUBES

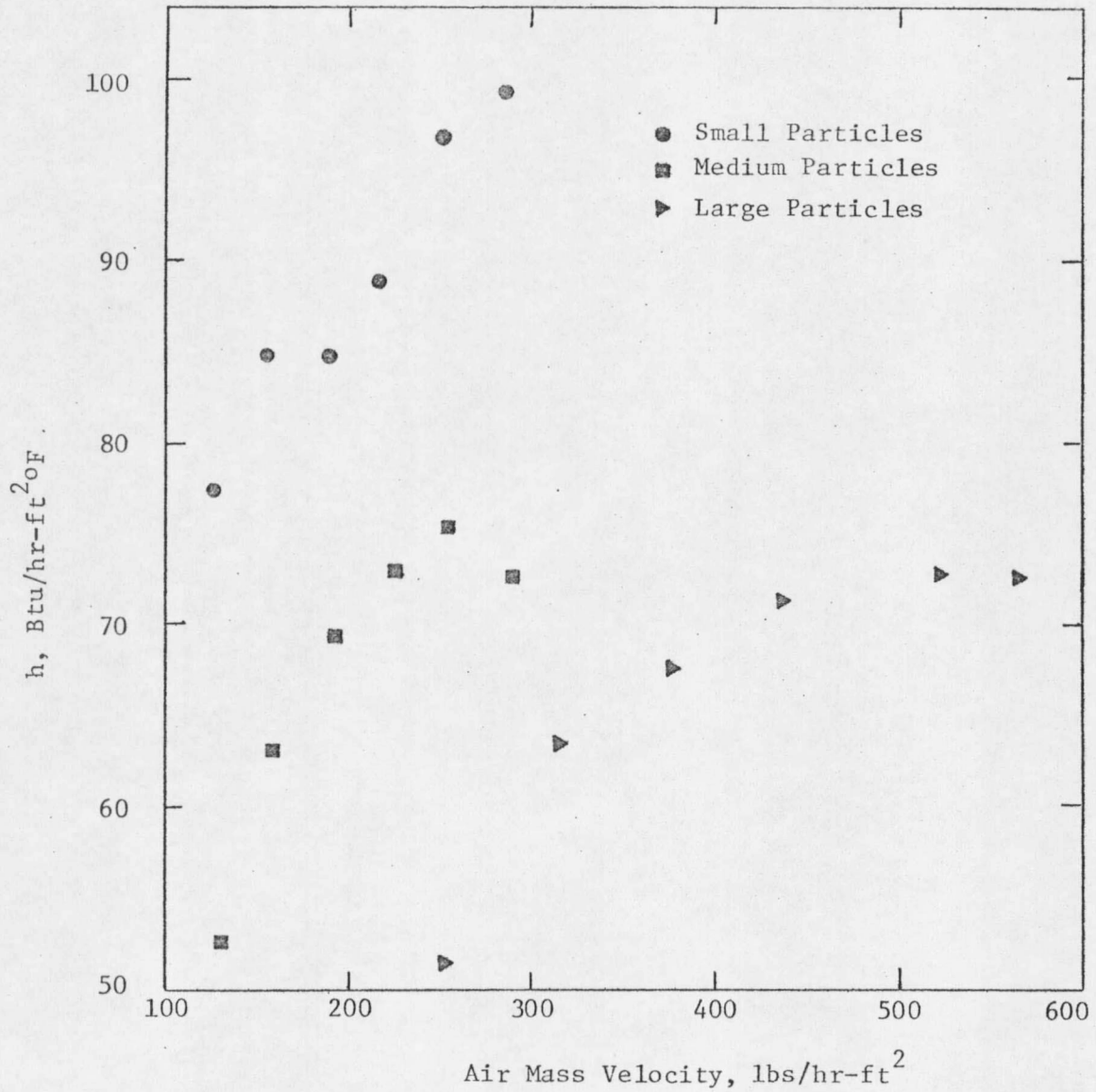


FIGURE 12.  $h$  VERSUS AIR MASS VELOCITY, #5 TUBES

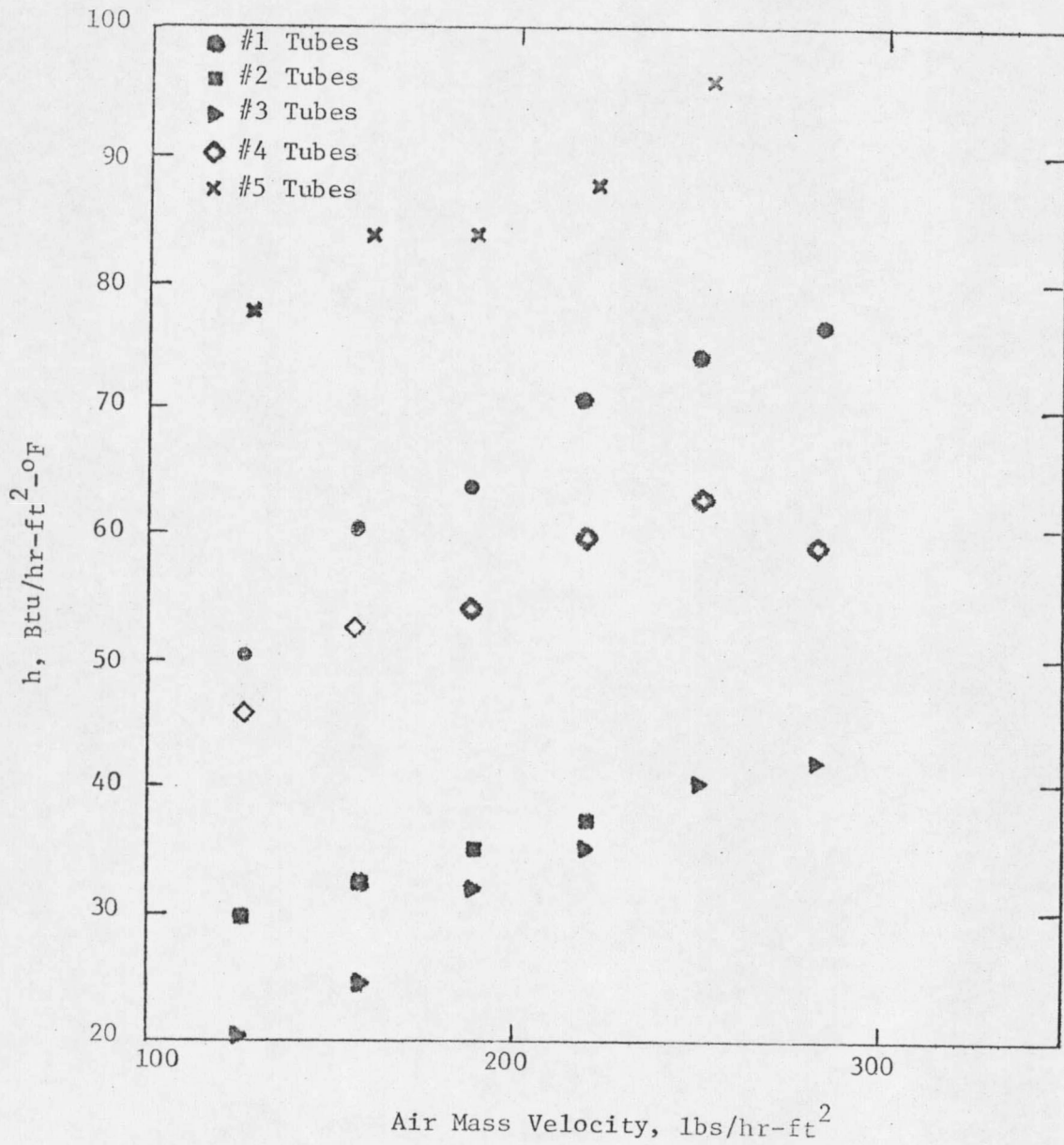


FIGURE 13. h VERSUS AIR MASS VELOCITY, SMALL PARTICLES

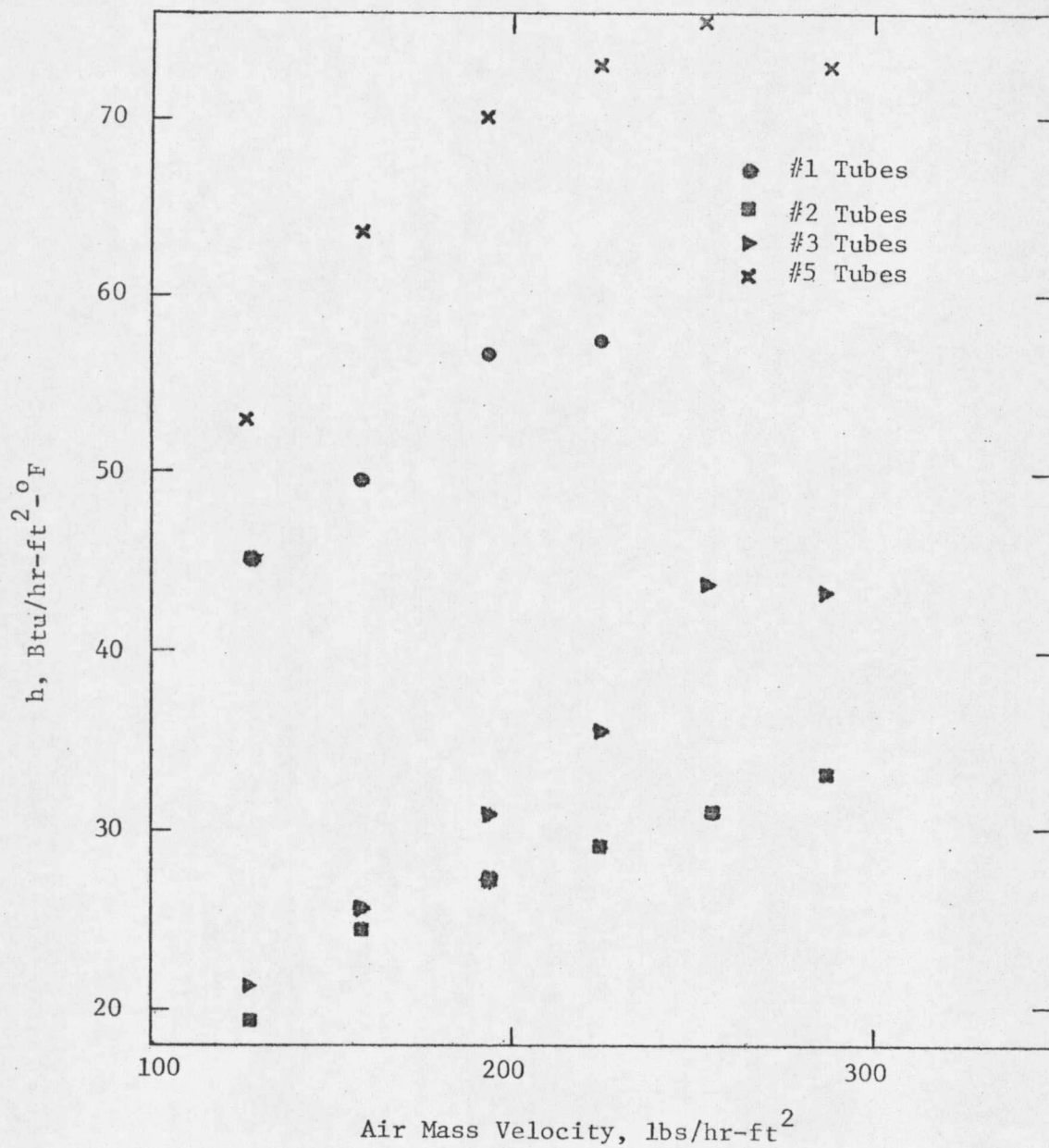


FIGURE 14.  $h$  VERSUS AIR MASS VELOCITY, MEDIUM PARTICLES

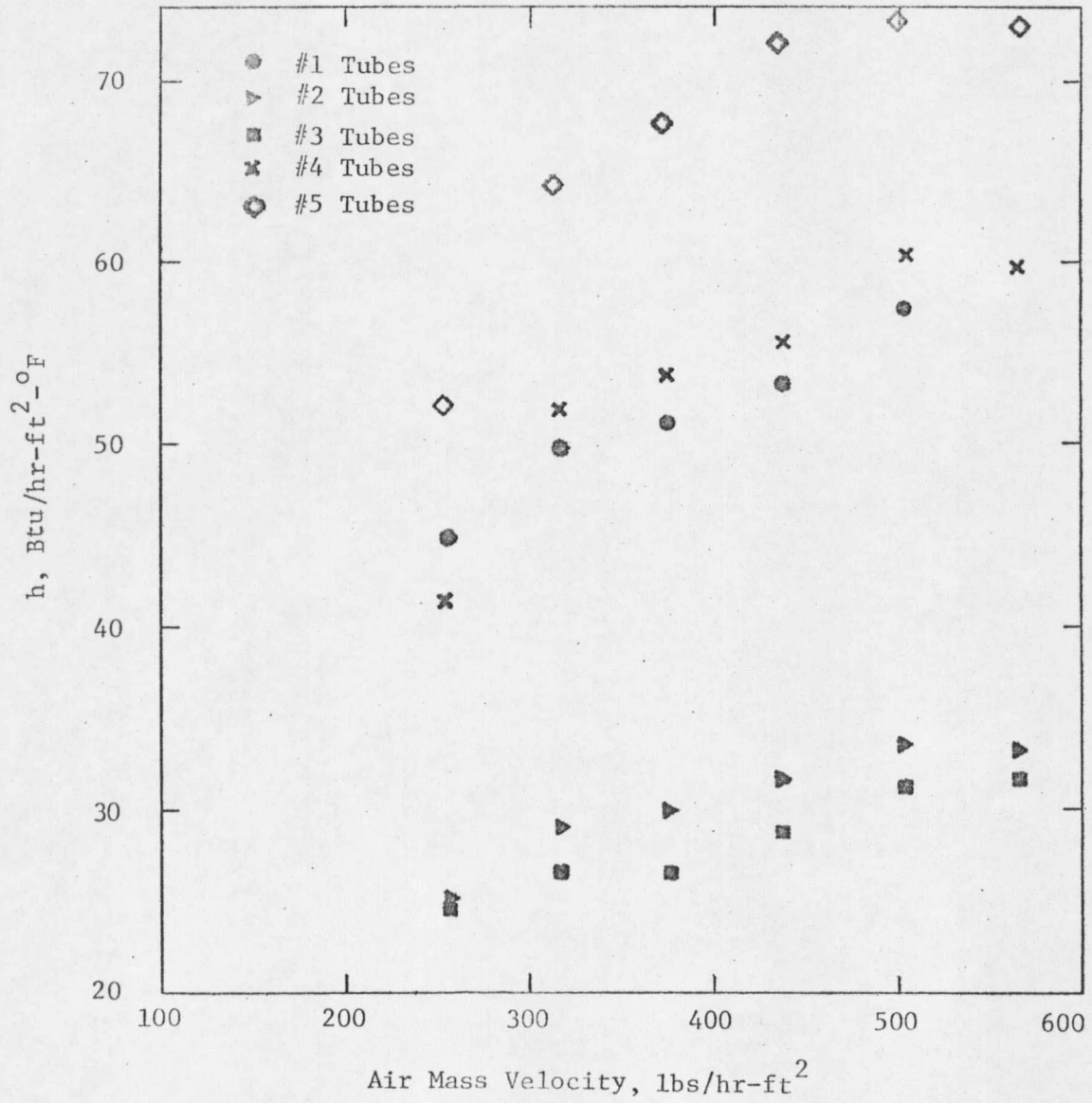


FIGURE 15. h VERSUS AIR MASS VELOCITY, LARGE PARTICLES

Performance of Finned Tubes

Since the reported heat transfer coefficients are based on the total area of the finned tubes, it is difficult to compare different tubes unless the areas are also presented. The most effective way is to compare the performance of the different tubes.

The performance is calculated using Equation 13.

$$P = \frac{(Q/\Delta T) \text{ Fin Tube}}{(Q/\Delta T) \text{ Bare Tube}} \quad (13)$$

p = Performance, dimensionless

Q = Heat transferred, Btu/hr

$\Delta T$  = Temperature driving force  $^{\circ}F$

The area of the bare tube, used to determine  $(Q/\Delta T)$  bare tube, is calculated using the 'overall fin diameter', (OFD). The OFD is defined as the tube diameter across the fin tips (see Figure 3). Using the OFD to calculate  $A_B$ , you are comparing the amount of heat transferred from the finned tube to the heat transferred from a bare tube occupying the same volume. The performance is the ratio of the heat transfer from an extended surface to a bare tube at the same temperature drop between the heat transfer surface and the bulk medium. The performances for each tube are shown in Figures 16, 17, 18, 19, and 20.

The performance increased with increasing mass flow rate. The

performance tends to increase with an increase in particle size. There is a larger difference in performance between the large particles and the medium particles than between the medium particles and the small particles.

For all the tubes there were some operating conditions where the performance value was less than 1. The low performance values were primarily at the lower mass velocities.

With the #4 tubes ( longest fins ) and the small particles, the performance was never greater than 1. The largest performance value of 1.74 occurred using the #1 tubes and the large particles. The #1 tubes have the largest fin spacing of the tubes. The #5 tubes also had a high performance (1.72). These tubes had the shortest fins and a larger fin separation.

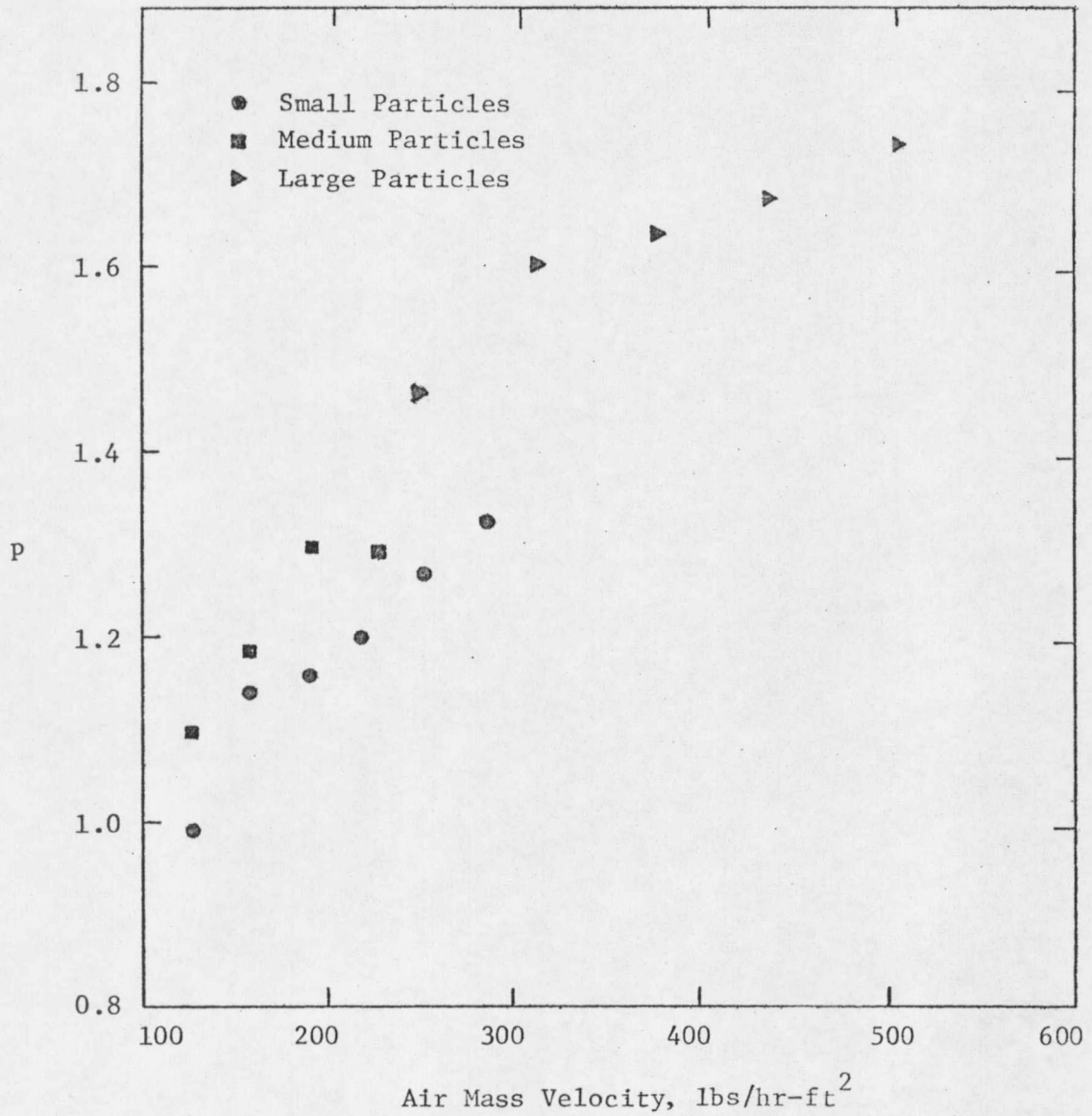


FIGURE 16. p VERSUS AIR MASS VELOCITY, #1 TUBES

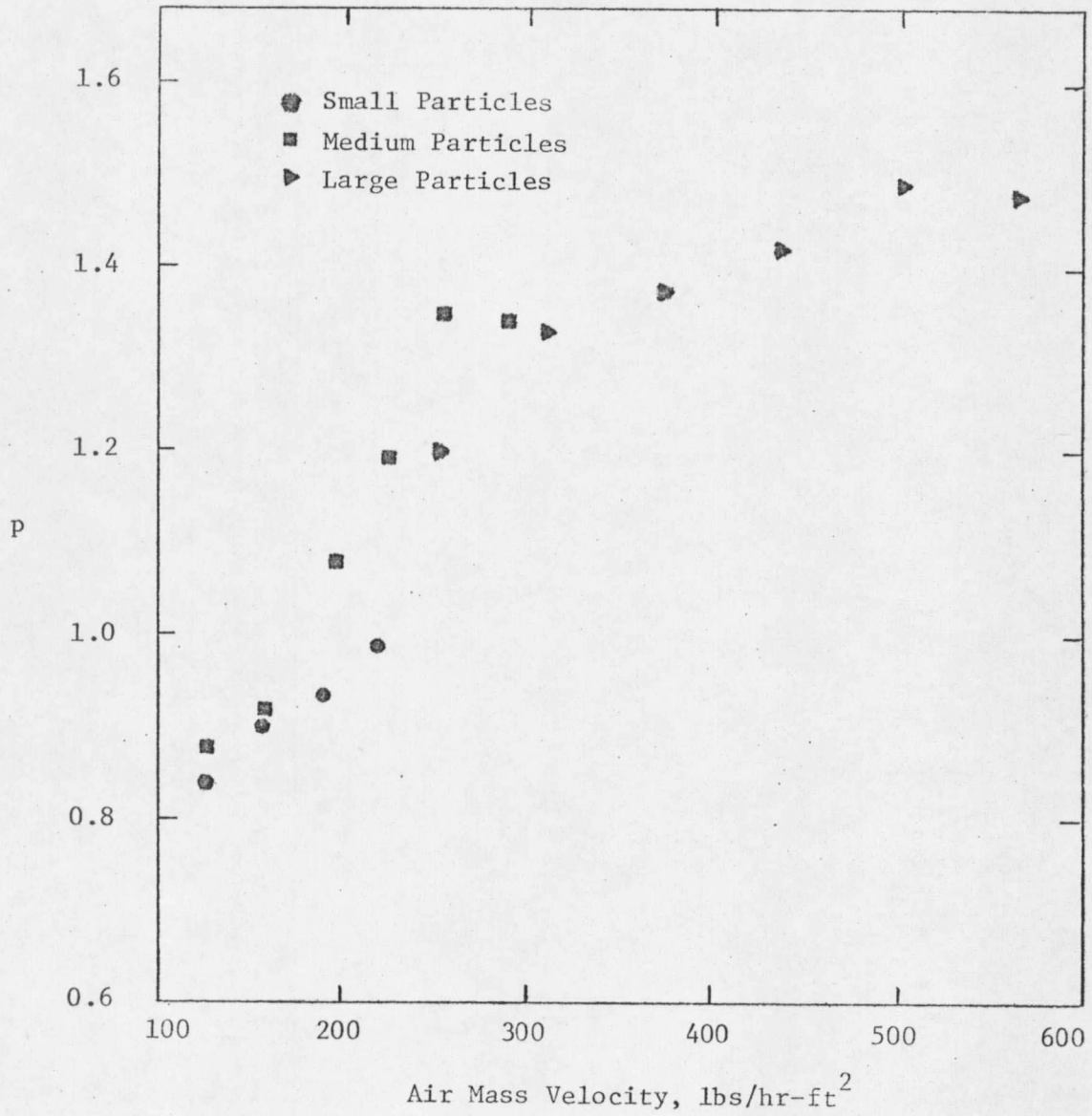


FIGURE 17. p VERSUS AIR MASS VELOCITY, #2 TUBES

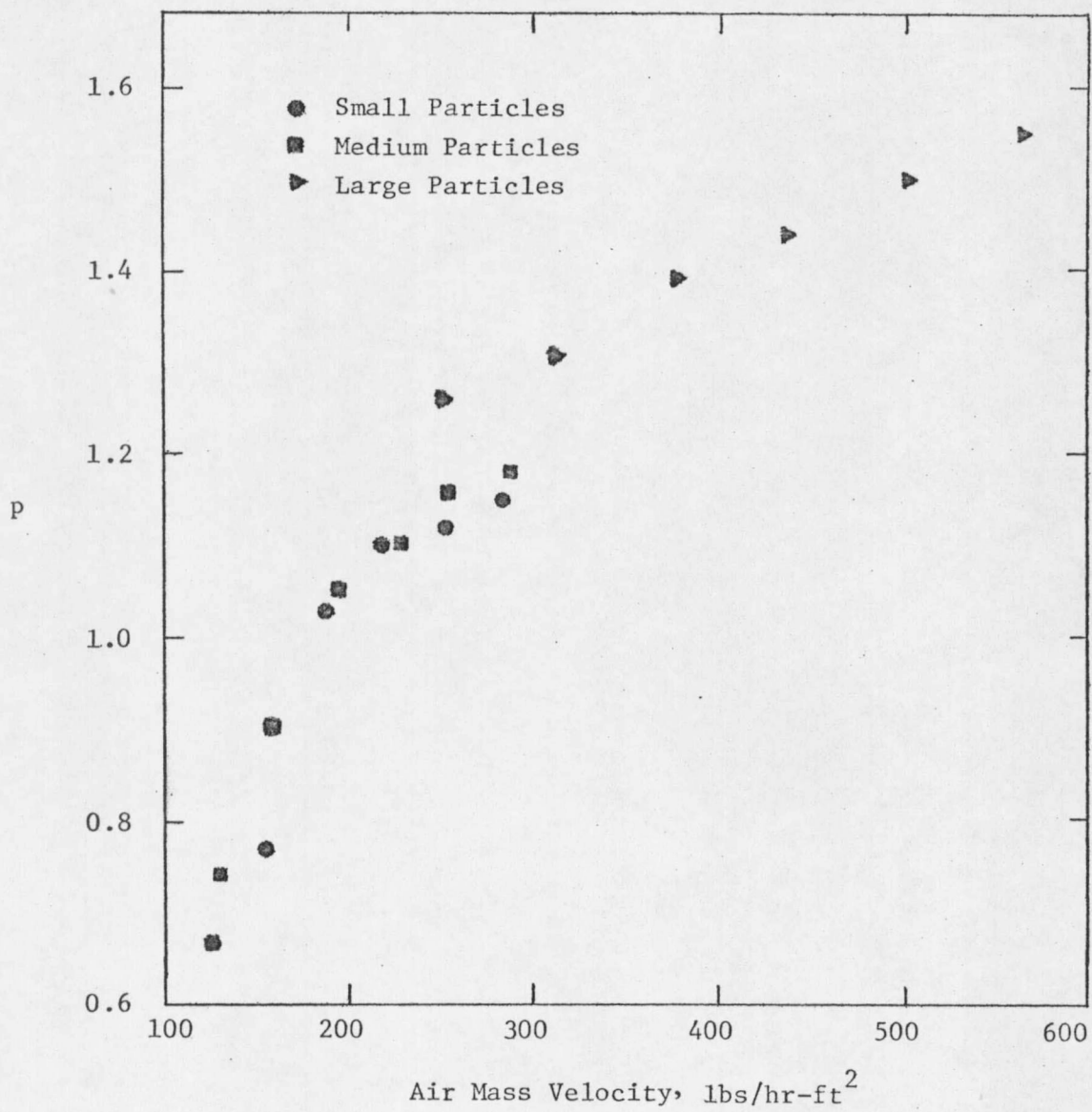


FIGURE 18. p VERSUS AIR MASS VELOCITY, #3 TUBES

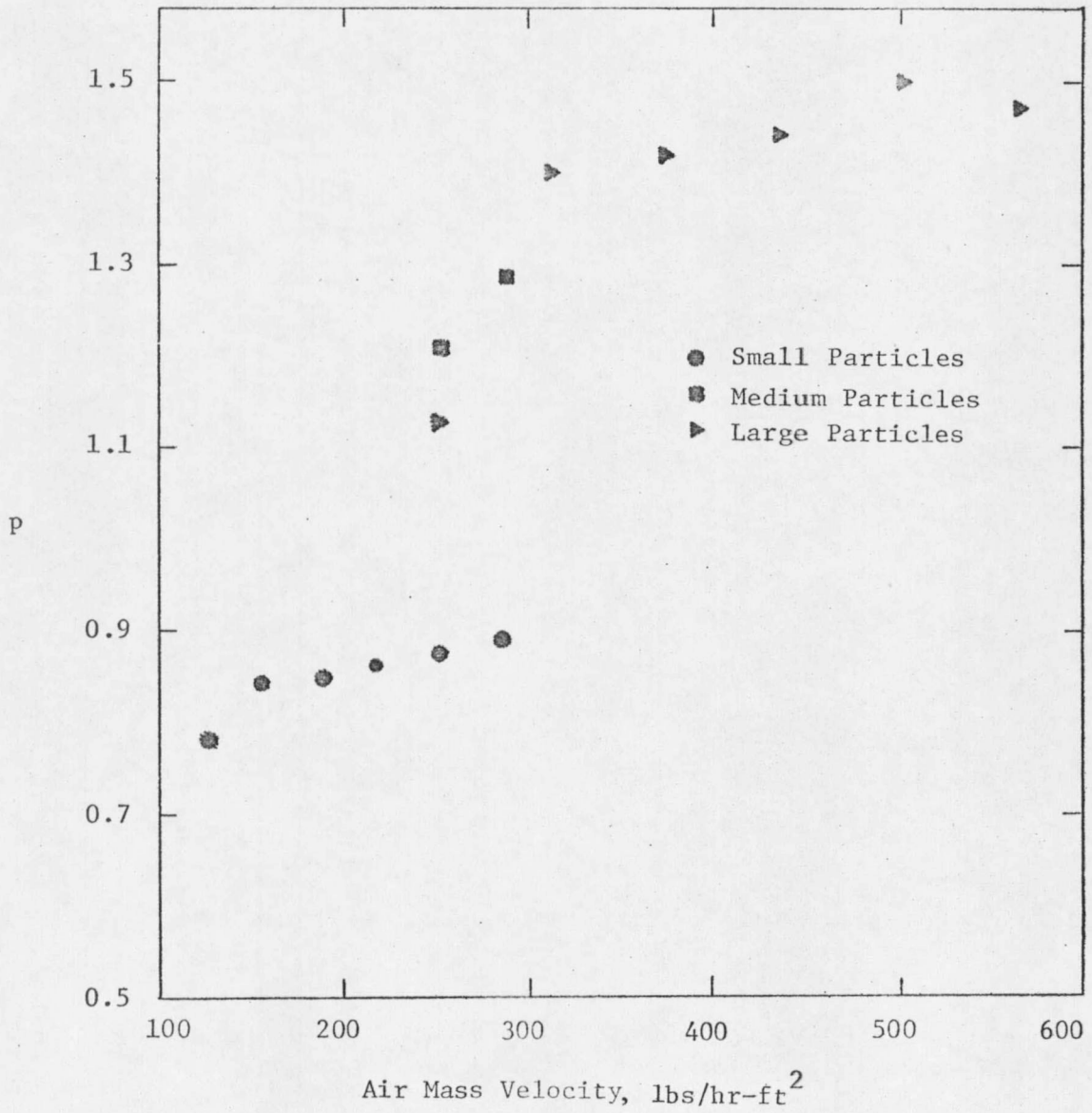


FIGURE 19.  $p$  VERSUS MASS FLOW RATE, #4 TUBES

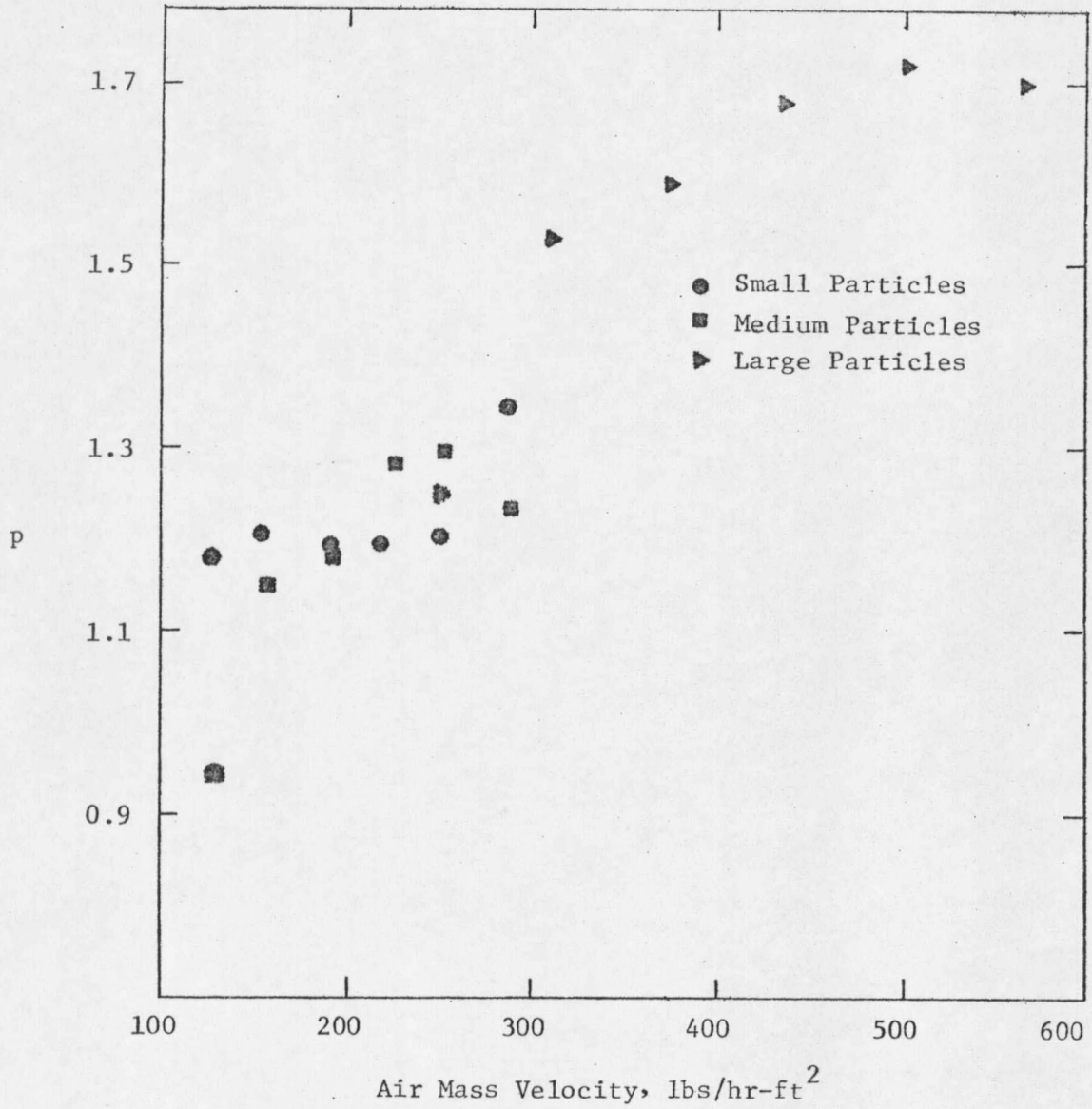


FIGURE 20. p VERSUS AIR MASS VELOCITY, #5 TUBES

## CONCLUSIONS

From this investigation the following conclusions were drawn:

1. Heat transfer coefficients increased with increasing air mass velocity. For some conditions a maximum was reached.
2. Heat transfer coefficients decreased with increasing particle size. The effect was greater between the large and medium particles than between the medium and small particles.
3. Heat transfer coefficients increased with increasing fin spacing.
4. Heat transfer coefficients decreased with increasing fin length.
5. Heat transfer coefficients increase with increasing fin separation.
6. Tube location did not affect the  $h$  values.
7. Performance increased with increasing mass velocity, increasing fin spacing and increasing fin separation.
8. Gains of up to 74% were obtained when compared to bare tubes.

## RECOMMENDATIONS

1. A further investigation with serrated fin tubes should be conducted with expanded experimental variables.
2. An investigation to determine the effect of fin separation on the heat transfer coefficients.

## ERROR ANALYSIS

Assuming the experimental heat transfer is only affected by the measurements of  $q$  and  $(T_w - T_b)$ , the error analysis is performed on equation 14.

$$h = \frac{q}{A_T (T_w - T_b)} \quad (14)$$

The wattmeter was assumed to be accurate within  $\pm 5$  percent. The bed temperature is assumed to be measured within  $\pm 0.5^\circ\text{F}$  and the tube wall temperature could be measured within  $\pm 1.5^\circ\text{F}$ . The minimum  $(T_w - T_b)$  value in this investigation was  $18.5^\circ\text{F}$ .

The maximum and minimum errors for  $h$  can be determined using the previous assumptions. This analysis is based on an  $h$  'true' value of 1.0.

### Maximum h

$$h = \frac{1.05}{1 - 2/18.5} = 1.18 \quad (15)$$

$$\text{Error} = (1.18 - 1.0) \times 100 = 18 \text{ percent}$$

### Minimum h

$$h = \frac{.95}{1 + 2/18.5} = .86 \quad (16)$$

$$\text{Error} = (.86 - 1.0) \times 100 = -14 \text{ percent}$$

The experimental error range is  $\pm 18$  percent,  $-14$  percent. The maximum deviations from the 'true' value should be  $\pm 18$  percent.

## CALCULATIONS

### Air Mass Velocity

For both blowers a 1.5 inch orifice with vena contracta taps and a water filled manometer were used to measure the air flow rates in the column. The following equation was used for the calculations (1):

$$G = \frac{3600 C_o Y S_c}{A_c} \frac{2 g_c (P_1 - P_2) \rho_1^{0.5}}{1 - \beta^4} \quad (17)$$

$G$  = Air Mass Velocity, lbs/hr-ft<sup>2</sup>

$C_o$  = Orifice Coefficient, Dimensionless

$Y$  = Expansion Factor, Dimensionless

$S_c$  = Cross Sectional Area of Orifice, ft<sup>2</sup>

$A_c$  = Cross Sectional Area of Column, ft<sup>2</sup>

$g_c$  = Gravitational Constant, ft-lb<sub>m</sub>/sec<sup>2</sup>-lb<sub>f</sub>

$P_1$  = Pressure at Upstream Pressure Tap, lb<sub>f</sub>/ft<sup>2</sup>

$P_2$  = Pressure at Downstream Pressure Tap, lb<sub>f</sub>/ft<sup>2</sup>

$\rho_1$  = Density of Air at the Upstream Pressure, lb<sub>m</sub>/ft<sup>3</sup>

$\beta$  = Ratio of Orifice Diameter to Inside Pipe Diameter  
Dimensionless

For a square edged orifice, the expansion factor is given as fol-

lows:

$$Y = 1 - \left[ \frac{P_1 - P_2}{P_1 K_r} (.41 - .35\beta^4) \right] \quad (18)$$

$$K_r = C_p / C_v$$

The orifice coefficient is a function of the Reynolds number. It was found to be nearly constant at 0.61 for both blowers for the range of air flow rates used.

#### Tube Temperatures

The tube temperatures were read directly using thermocouples connected to a Brown Potentionmeter.

#### Bed Temperature

The bed temperature,  $T_b$ , was the average of the three bed thermocouple readings.

#### Heat Input to Each Tube

The power to each tube was measured with a wattmeter and then converted to the appropriate units.

$$q = (\text{Watts}) \frac{3.4129 \text{ Btu}}{\text{Watt-hr}} \quad (19)$$

#### Total Tube Area

The total fin area was found by multiplying the area per fin by the number of fins. The total tube area was calculated by adding the total fin area and the area of the unfinned portion of the tube. The average of the 7 tubes was used in the calculations.

### Air Thermal Conductivity

The air thermal conductivity,  $k_g$ , was determined by linear interpolation between the values listed in Kreith (10). The evaluation temperature was the bed temperature,  $T_b$ .

### Air Viscosity

The air viscosity was calculated for each bed temperature from the following equation which was fit to experimental data (9):

$$\mu_g = (2.45 (T_b - 32) + 1538.1) 2.688 \times 10^{-5} \quad (20)$$

$\mu_g$  = Air Viscosity, lb/hr-ft

$T_b$  = Bed Temperature, °F

### Heat Transfer Coefficient

The heat transfer coefficients were calculated using the following equation:

$$h = \frac{q}{A_b (T_w - T_b) + A_F (T - T_b)} \quad (21)$$

$h$  = Heat Transfer Coefficient, Btu/hr-ft<sup>2</sup>-°F

$q$  = Heat Input Per Tube, Btu/hr

$A_b$  = Unfinned Area of Tube, ft<sup>2</sup>

$A_F$  = Finned Area of Tube, ft<sup>2</sup>

$T_w$  = Tube Wall Temperature, °F

$T_b$  = Bed Temperature, °F

$(T - T_b)_{MF}$  = Mean Temperature Difference, °F

Particle Nusselt Number

$$Nu_p = \frac{h D_p}{k_g} \quad (22)$$

$Nu_p$  = Nusselt Number, Dimensionless

$h$  = Heat Transfer Coefficient, Btu/hr-ft<sup>2</sup>°F

$D_p$  = Particle Diameter, ft

$k_g$  = Air Thermal Conductivity, Btu/hr-ft<sup>2</sup>°F

Particle Reynolds Number

$$Re_p = \frac{G D_p}{\mu_g} \quad (23)$$

$Re_p$  = Particle Reynolds Number, Dimensionless

$G$  = Air Mass Velocity, lbs/hr-ft<sup>2</sup>

$D_p$  = Particle Diameter, ft

$\mu_g$  = Air Viscosity, lbs/hr-ft

NOMENCLATURE

	<u>Definition</u>	<u>Units</u>
$A_D$	Bare Tube Area	$\text{ft}^2$
$A_C$	Cross Sectional Area of Column	$\text{ft}^2$
$A_F$	Area of Fins	$\text{ft}^2$
$A_T$	Total Area	$\text{ft}^2$
$C_O$	Orifice Coefficient	Dimensionless
$C_{P_S}$	Heat Capacity of Solids	$\text{Btu/lb-}^\circ\text{F}$
$D_P$	Particle Diameter	Inches
$G$	Air Mass Velocity	$\text{lbs/hr-ft}^2$
$g_c$	Gravitational Constant	$\text{ft-lb/hr}^2\text{-lb}_P$
$h$	Heat Transfer Coefficient	$\text{Btu/hr-ft}^2\text{-}^\circ\text{F}$
$k$	Thermal Conductivity	$\text{Btu/hr-ft-}^\circ\text{F}$
$k_g$	Thermal Conductivity of Fluidizing Mass	$\text{Btu/hr-ft-}^\circ\text{F}$
$L$	Fin Length	Inches
$N_t$	Number of Fins	Dimensionless
$N$	Particle Nusselt Number	Dimensionless
$OFD$	Overall Fin Diameter	Inches
$p$	Performance	Dimensionless
$q, Q$	Rate of Heat Transfer	$\text{Btu/hr}$
$R$	Particle Reynolds Number	Dimensionless
$S_c$	Cross Sectional Area of Orifice	$\text{ft}^2$
$T_b$	Bed Temperature	$^\circ\text{F}$

	<u>Definition</u>	<u>Units</u>
$T_s, T_w$	Surface or Wall Temperature	$^{\circ}\text{F}$
$(T - T_b)_{MF}$	Mean Temperature Difference Between Fin and Bed	$^{\circ}\text{F}$
$v$	Fin Thickness	ft
$w$	Fin Width	ft
$Y$	Expansion Factor	Dimensionless
$\beta$	Ratio of Orifice Diameter to Pipe Diameter	Dimensionless
$1 - \epsilon$	Particle Fraction	Dimensionless
$\bar{\theta}$	Average Contact Time	hr
$\rho_l$	Density of Fluidizing Mass	$\text{lb}/\text{ft}^3$
$\rho_s$	Density of Solids	$\text{lb}/\text{ft}^3$
$\mu_g$	Viscosity of Fluidizing Mass	$\text{lb}/\text{ft}\text{-hr}$

## BIBLIOGRAPHY

1. Perry, R.H., Chemical Engineers' Handbook, 4th Edition, McGraw-Hill Book Co., New York, 1973.
2. Levenspiel, O., Chemical Reaction Engineering, John Wiley and Sons, Inc., New York, 1963.
3. Mickley, H.S., and D.F. Fairbanks, A.I.Ch.E. Journal, 1, 374(1955).
4. Ziegler, E.N., L.B. Koppel, and W.T. Brazelton, Ind. Eng. Chem. Fundamentals, 3, 324(1964).
5. Genetti, W.E., and J.G. Knudsen, I. Chem. Eng. Symp. Series, 30, 147(1968).
6. Kunii, D., and O. Levenspiel, Fluidization Engineering, John Wiley and Sons, Inc., New York, 1969.
7. Chen, J.C. and J.G. Withers, "An Experimental Study of Heat Transfer from Plain and Finned Tubes in Fluidized Beds", A.I.Ch.E. Paper No. 34, 15th National Heat Transfer Conference, San Francisco(1975).
8. Chen, J.C., "Heat Transfer to Tubes in Fluidized Beds", A.S.M.E. Paper No. 76-HT-75, 16th National Heat Transfer Conference, St. Louis(1976).
9. Everly, D.W., M.S. Thesis, Montana State University(1978).
10. Kreith, F., Principles of Heat Transfer, Intext Press, Inc., New York, 1973.

MONTANA STATE UNIVERSITY LIBRARIES



3 1762 10020819 6

~~N278  
V284  
Cap 2~~